



Theoretical study of materials from first principles

Samuel Quintero González



Supervised by:

Dr. Andrés Mujica Fernaud

Dr. Silvana Radescu Cioranescu

Academic year: **2018/2019**



Contents

| | | |
|----------|--|-----------|
| 1 | Introduction | 4 |
| 2 | Fundamental concepts and definitions | 5 |
| 2.1 | The Bravais lattice | 5 |
| 2.2 | The reciprocal lattice | 5 |
| 2.3 | Periodic potentials in one dimension | 7 |
| 3 | Theoretical background | 11 |
| 3.1 | The Born-Oppenheimer approximation | 11 |
| 3.2 | The electron density | 11 |
| 3.3 | The Hohenberg-Kohn theorem(s) | 12 |
| 3.4 | The Kohn-Sham equations | 14 |
| 3.5 | Approximation methods | 15 |
| 3.5.1 | Local density approximation (LDA) and generalized gradient approximation (GGA) | 15 |
| 3.5.2 | The plane waves (PW) and the orthogonal plane waves (OPW) method | 16 |
| 3.5.3 | The pseudopotential method | 19 |
| 4 | Ab initio calculations for selected materials | 20 |
| 4.1 | Introduction | 20 |
| 4.2 | Methodology | 20 |
| 4.3 | Details of the calculations | 22 |
| 4.4 | Results and analysis | 23 |
| 4.4.1 | Equations of state | 23 |
| 4.4.2 | Electronic energy bands | 26 |
| 4.4.3 | Electronic localization function (ELF) | 28 |
| 5 | Conclusions | 30 |
| A | Appendix | 31 |
| A.1 | Table of atomic units | 31 |
| A.2 | Bloch's theorem for the multidimensional case | 31 |
| A.3 | Some explicit calculations related to the electron density | 32 |
| A.4 | Derivation of the Kohn-Sham equations | 35 |

Acknowledgments

I would like to express my special gratitude to Andrés Mujica and Silvana Radescu, whose contributions in suggestions and support, helped me to coordinate my project especially in writing this memory. I would also like to thank my mother and siblings for their continuous support along these years. And last, but not least, thanks to Alba for her countless suggestions to improve this work and all her support during the course of this project.

Abstract

Este trabajo se centra en el estudio del formalismo del funcional densidad (DFT), y en él hacemos un gran énfasis en cómo la estructura de un material tienen un gran impacto en sus propiedades. A modo de ejemplo, se proporciona una sencilla demostración de la existencia de bandas en el espectro del Hamiltoniano para sistemas unidimensionales cuando el potencial es periódico. A continuación, se demuestran los dos grandes teoremas de la DFT. Estos teoremas, junto al *ansatz* de Kohn and Sham y el principio variacional de la mecánica cuántica, conducen a las llamadas ecuaciones de Kohn y Sham. Seguidamente se discuten varios de los métodos de aproximación más usuales para resolver computacionalmente las mencionadas ecuaciones. Todos estos métodos descritos, o versiones más elaboradas de ellos, aparecen implementados en rutinas del programa VASP, el cual utilizamos en este trabajo a fin de realizar cálculos para el diamante y el grafito. En concreto estudiamos las curvas de energía-volumen para ambas fases del carbono, y las ajustamos a ecuaciones de estado. También se calculan las bandas de energía a distintas presiones de ambos materiales y se estudia la evolución del *gap* del diamante. Para finalizar se introduce la función de localización electrónica, la cual permite visualizar las zonas con mayor probabilidad de localización de electrones.

1 Introduction

Since the discovery of the electron as a carrier of negative charge, physicists have tried to determine its importance in the properties of a material. The first attempt was due to Drude (1900), when he proposed a classical model where the electrons in metals were only scattered because of nuclei and did not interact among themselves. Despite being so simple, this model predicts several properties of metals, as their conductivity or their resistance. However, it fails to predict the dependence of these properties with a magnetic field, but its predictions work as limiting values for some magnitudes. The most remarkable feature of Drude's model is that all of its magnitudes depend on the electronic density, which characterizes the material. Even if this model is classical, this electronic density plays an fundamental role.

With the arrival of Quantum Mechanics, specifically with the discovery Schrödinger equation (1925), a model of free electrons for the electrons of metals is proposed, whose main properties, such as the Fermi energy, depend once again on the electronic density. Later on, the Dirac-Fermi statistics is introduced, which takes into account that not all electrons excited with an external excitation due to Pauli exclusion principle, and the only electrons that respond to this field will be those near to the so called Fermi surface, as the occupancy of their energies is less than one. And precisely this Fermi surface does also depend on the electronic density. Therefore, it appears that the density is something more important than it was suspected at the beginning. At this point, it was just a matter of time to produce a full quantum mechanical theory in which the density is the main variable defining the properties of the system, and that theory is the density functional theory (DFT) of Hohenberg, Kohn and Sham of 1965.

To sum up, in this memory we will see that the recurrent appearance of the electronic density has a central role in order to explore and explain the properties of the materials. We will see that all the properties of a material depend on its ground state electronic density.

2 Fundamental concepts and definitions

2.1 The Bravais lattice

Crystallography studies crystalline matter, i.e, arranged in a periodic array. There is interest on how the properties of a crystalline solid emerge from its underlying crystal structure. One example of this is diamond and graphite, which are both, with very different structure and properties, made of carbon (C)

The concept of Bravais lattice is introduced to model this periodic arrangement. We define a **Bravais lattice** as “an infinite array of discrete points with an arrangement and orientation that appears exactly the same, from whichever of the points the array is viewed” ([5], p.64). And precisely on this mesh is where identical groups of atoms are placed, named as the **basis** of the lattice. In fact, we can define more precisely a Bravais lattice as the set of points with position vector \vec{R} of the form:

$$\vec{R} = n_1\vec{a} + n_2\vec{b} + n_3\vec{c} \quad n_i \in \mathbb{Z} \quad (2.1)$$

where $\{\vec{a}, \vec{b}, \vec{c}\}$ form a so called set of lattice generators. From now on we will denote this set as \mathbf{R} . The parallelepiped spanned by these vectors is a **unit cell** of the lattice. A cell is called **primitive** if it contains only one lattice point, so its volume is minimum with respect to other choices of the cell. The vectors that span this primitive cell are called **primitive generators**. By convention, the reference system is chosen in such a way that if the atoms are inside the cell their coordinates with respect to primitive generators will be less or equal to one.

The norms (a, b, c) and relative angles (α, β, γ) of these vectors are used in order to classify the Bravais lattice cells into seven crystal system (see Figure 1). One can always choose a primitive cell with the full symmetry of the Bravais lattice, the **Wigner-Seitz primitive cell**. This cell is constructed by considering the region around a lattice point that is closer to that point than to any other lattice point.

Even so there are other ways to classify them. For instance, we could introduce a classification in terms of the symmetry elements of the lattice. This is useful for computational purposes, as from a small portion of the cell one can reconstruct the entire cell using the symmetry operators, see ref. [14].

2.2 The reciprocal lattice

The first section introduces the concept of Bravais lattice which from now on will be called **direct lattice**. The periodic arrangement is in the origin of the periodic potential and also on the symmetry properties of the wave function, through Bloch’s theorem. For computational purposes, we are interested in the electronic Fourier expansion of periodic quantities:

$$f(\vec{r}) = \sum_{j=0}^{\infty} c_j \cdot e^{i\vec{k}_j \cdot \vec{r}} \quad (2.2)$$

In order for to $f(\vec{r})$ be periodic, i.e. $f(\vec{r}) = f(\vec{r} + \vec{R})$ for all $\vec{R} \in \mathbf{R}$, only certain wave vectors \vec{k}_j are allowed. The exponential in [2.2] must have the periodicity of the lattice:

$$e^{i\vec{k}_j \cdot (\vec{r} + \vec{R})} = e^{i\vec{k}_j \cdot \vec{r}} \iff \vec{k}_j \cdot \vec{R} = 2\pi \quad \forall \vec{R} \in \mathbf{R} \quad (2.3)$$

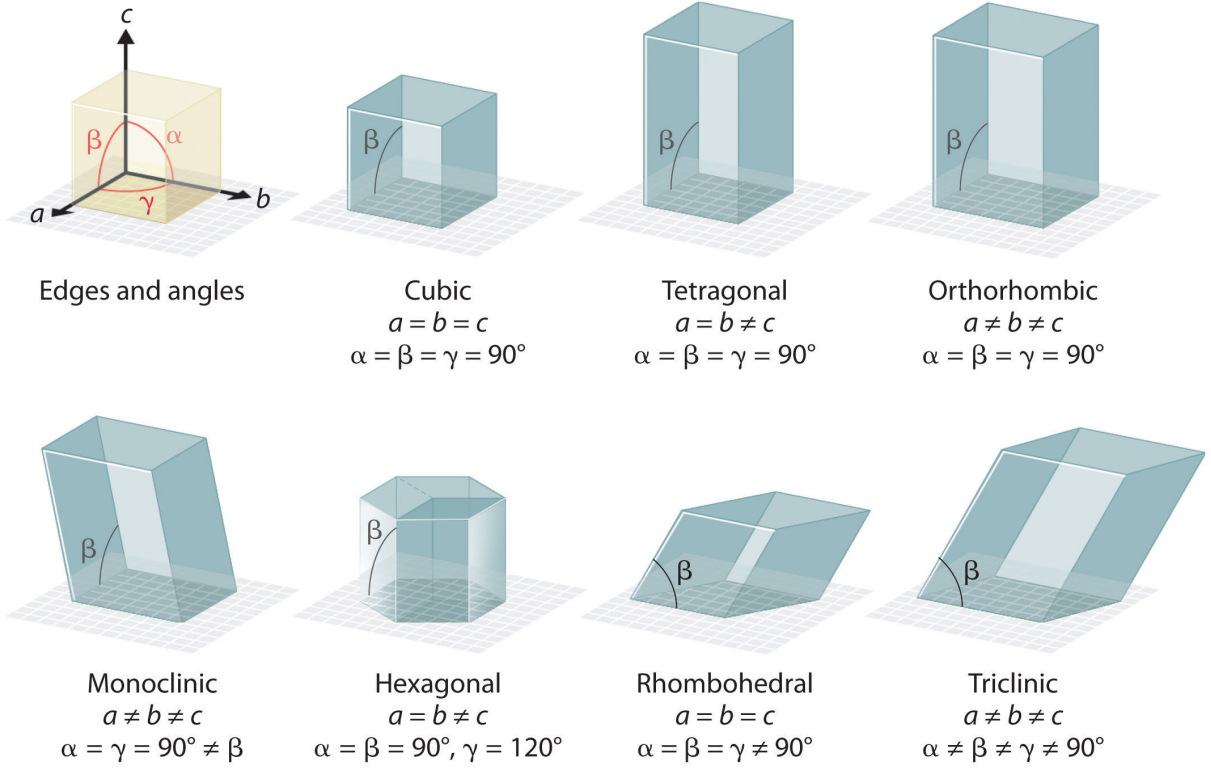


Figure 1: Classification of Bravais lattice [6]

If we define the **reciprocal lattice generators** (\vec{b}_i) as:

$$\vec{b}_1 := \frac{2\pi}{\Omega} \cdot (\vec{a}_2 \times \vec{a}_3) \quad \vec{b}_2 := \frac{2\pi}{\Omega} \cdot (\vec{a}_3 \times \vec{a}_1) \quad \vec{b}_3 := \frac{2\pi}{\Omega} \cdot (\vec{a}_1 \times \vec{a}_2) \quad (2.4)$$

with $\Omega = \vec{a}_1 \cdot (\vec{a}_2 \times \vec{a}_3)$, i.e. the volume of the parallelepiped formed by the \vec{a}_i vectors of the primitive unit cell, it is easily shown that $\vec{a}_i \cdot \vec{b}_j = 2\pi\delta_{ij}$. If we span the wave vectors \vec{k}_i in this basis:

$$\vec{k}_i = k_{1i} \vec{b}_1 + k_{2i} \vec{b}_2 + k_{3i} \vec{b}_3 \quad (2.5)$$

From equation [2.3] it follows that k_{ji} should be integers. The set of all wave vectors satisfying [2.5] is a Bravais lattice, named the **reciprocal lattice**, whose primitive vectors are \vec{b}_i . From now on we will denote the reciprocal lattice as \mathbf{R}^* . Equation [2.2] can be rewritten as:

$$f(\vec{r}) = \sum_{\vec{k} \in \mathbf{R}^*} c_{\vec{k}} \cdot e^{i\vec{k} \cdot \vec{r}} \quad (2.6)$$

The Wigner-Seitz primitive cell of the reciprocal lattice is called the **first Brillouin zone (FZB)**.

For the wavefunctions, which are Bloch functions, it is usual to choose **Born-von Kármán boundary conditions** or periodic boundary conditions (PBC), which consist in enclosing the system into a parallelepiped of dimensions $N_1 \times N_2 \times N_3$ with the integers N_i large enough, and impose periodic boundary conditions on it:

$$\psi(r_1 + N_1 R_1, r_2 + N_2 R_2, r_3 + N_3 R_3) = \psi(\vec{r}) \quad (2.7)$$

where $\{r_i\}_{i=1}^3$ are the components of the position vector \vec{r} . Then, the wave vectors can be expanded as:

$$\vec{k} = \sum_{i=1}^3 \left(\frac{m_i}{N_i} \right) \cdot \vec{b}_i \quad m_i \in \mathbb{Z} \quad (2.8)$$

and the plane waves expansion [2.6] for ψ follows.

2.3 Periodic potentials in one dimension

We have already seen that crystalline matter is modeled as an infinity array of cells where groups of atoms are placed, but what are the physical implications of such an arrangement? We will see that the symmetry of the lattice is in the origin of energy bands in the spectrum of the Hamiltonian, also called Schrodinger operator, of the system. We will now show this for a one dimensional lattice, see ref. [15]. The Hamiltonian we are going to consider in this section is:

$$\hat{H} = -\frac{\hbar^2}{2m} \cdot \frac{d^2}{dx^2} + V(x) \quad (2.9)$$

where the potential $V(x)$ satisfies:

- $V(x + a) = V(x)$ where a is the spatial periodicity of the 1D-lattice.
- $V(x)$ is a piece-wise continuous and bounded function.

The standard approach to this problem is to solve the eigenstate equation of the Hamiltonian:

$$\hat{H}\psi(x) = E\psi(x) \longrightarrow -\frac{\hbar^2}{2m} \frac{d^2\psi}{dx^2} + V(x)\psi(x) = E\psi(x) \quad (2.10)$$

But in order to use many of the results of the ODE calculus we must admit complex eigenvalues for the equation: $E \in \mathbb{C}$. We need to see equation [2.10] not as an eigenvalue problem but rather as a differential equation problem, and at the end we will extract the physical implication by restricting E to the real line.

The point of all this section is to show that the spectrum of the Schrödinger operator has a band structure. For this, we will need to introduce some useful concepts and theorems, but not all of them will be proven because of the limited scope of this work.

From the general theory of ODE we know that there exists two fundamental solutions, namely: $\psi_1^E(x)$ and $\psi_2^E(x)$, and any other solution can be expressed as a linear combination of these fundamental solutions:

$$\psi^E(x) = \sum_{i=1}^2 A^i \psi_i^E(x) \quad A^i \in \mathbb{C} \quad (2.11)$$

The initial conditions for the fundamental solutions are chosen conveniently as:

$$\left. \begin{aligned} \psi_1^E(0) &= 1 & \frac{d\psi_1^E}{dx} \Big|_{x=0} &= 0 \\ \psi_2^E(0) &= 0 & \frac{d\psi_2^E}{dx} \Big|_{x=0} &= 1 \end{aligned} \right\} \quad (2.12)$$

Theorem. ψ_1^E, ψ_2^E are entire functions¹ of E (at a fixed x). Also, the derivative of the fundamental solutions are entire functions.

We will see that this theorem is the key to prove that the spectrum have gaps of forbidden energies because of the continuity restriction on ψ_1^E and ψ_2^E .

Definition. The fundamental matrix of the ODE is:

$$M(x, E) := \begin{pmatrix} \psi_1^E(x) & \psi_2^E(x) \\ \frac{d\psi_1^E}{dx}(x) & \frac{d\psi_2^E}{dx}(x) \end{pmatrix} \quad (2.13)$$

The determinant of the fundamental matrix is known in the literature as **the Wronskian** of the ODE, and for equation [2.10] it is constant rather than a function of E or x .

Proof. We are going to show that : $[det(M(x, E))]' = 0$. The Wronskian is:

$$det(M(x, E)) = \psi_1^E(x) \cdot \frac{d\psi_2^E}{dx}(x) - \frac{d\psi_1^E}{dx}(x) \cdot \psi_2^E(x) \quad (2.14)$$

and the derivative:

$$\begin{aligned} [det(M(x, E))]' &= \frac{d\psi_1^E}{dx}(x) \cdot \frac{d\psi_2^E}{dx}(x) + \psi_1^E(x) \cdot \frac{d^2\psi_2^E}{dx^2}(x) - \frac{d^2\psi_1^E}{dx^2}(x) \cdot \psi_2^E(x) - \frac{d\psi_1^E}{dx}(x) \cdot \frac{d\psi_2^E}{dx}(x) = \\ &= -\frac{2m}{\hbar^2} \psi_1^E(x) \cdot (E - V(x)) \cdot \psi_2^E(x) + \frac{2m}{\hbar^2} \cdot (E - V(x)) \cdot \psi_2^E(x) \cdot \psi_1^E(x) = 0 \end{aligned}$$

Using equation [5]

(2.15)

Then, the Wronskian is a constant, in particular, $det(M(x, E)) = cte = det(M(0, E)) = 1$. We will see later that the determinant is important to evaluate the spectrum of the translation operator.

At least for now we are not using the fact that the potential is periodic, so this result is completely general in the sense that it does not depend on the choice of potential. We are going to use this piece of information now. If $\psi^E(x)$ is a solution then $\phi^E(x) = \psi^E(x + a)$ is solution too because of the translational symmetry. This does not mean $\psi^E(x) = \phi^E(x)$, only that both functions are solution of the same differential equation. How are both solutions related to each other? Recall that any solution can be expanded in terms of the fundamental solutions, thus:

$$\psi^E(x + a) = \sum_{i=1}^2 a^i \cdot \psi_i^E(x) \quad (2.16)$$

In particular, this is valid for the shifted fundamental solution $\psi_j^E(x + a)$:

$$\psi_j^E(x + a) = \sum_{i=1}^2 a^i \cdot \psi_i^E(x) \quad (2.17)$$

To calculate this coefficients let's consider the j shifted fundamental solution and its derivative evaluated at $x = 0$:

$$\psi_j^E(a) = a^1_j \cdot \psi_1^E(0) + a^2_j \cdot \psi_2^E(0) \quad (2.18)$$

¹An **entire function** is a differentiable function on the complex plane.

$$\frac{d\psi_j^E}{dx}(a) = a_j^1 \cdot \frac{d\psi_1^E}{dx}(0) + a_j^2 \cdot \frac{d\psi_2^E}{dx}(0) \quad (2.19)$$

We see that this is nothing else than the component of the fundamental matrix evaluated at $x = a$:

$$a_j^i = M_j^i(a, E) \quad (2.20)$$

Thus, a general shifted solution can be expanded in terms of the fundamental solutions as:

$$\psi^E(x + a) = \sum_{l=1}^2 A^l \psi_j^E(x + a) = \sum_{l=1}^2 \sum_{i=1}^2 A^l M_l^i(a, E) \psi_j^E(x) \quad (2.21)$$

A standard strategy to solve eigenvalue problems is to find commuting operators and solve simultaneously both eigenvalue equations. In view of the symmetry of the system one proposes the translation operator defined as:

$$T\psi(x) = \psi(x + a) \quad (2.22)$$

By direct calculation we see that $[T, H] = 0$. Therefore T and H have common eigenvectors that we are going to denote as $\psi^{E\lambda}(x)$. Then, we are solving simultaneously the equations:

$$H\psi^{E\lambda}(x) = E\psi^{E\lambda}(x) \quad (2.23)$$

$$T\psi^{E\lambda}(x) = \lambda\psi^{E\lambda}(x) \quad (2.24)$$

The elements of the family $\{\psi^{E\lambda}\}_{E \in \mathbb{C}}^{\lambda \in \mathbb{C}}$ are called **Bloch functions**.

Floquet's theorem. Any Bloch function has the form:

$$\psi^{E\lambda}(x) = \lambda^{x/a} \phi^E(x) \quad \text{where: } \phi^E(x + a) = \phi^E(x) \quad (2.25)$$

We want bounded solutions of the differential equation, so λ must be a pure phase, i.e:

$$\lambda = e^{i\theta} \quad \text{which } \theta \in (-\pi, \pi] \quad (2.26)$$

In the physics literature the wave number (k) is commonly used instead of θ :

$$k := \theta/a \longrightarrow k \in \left(-\frac{\pi}{a}, \frac{\pi}{a}\right] \quad (2.27)$$

In later discussion, we will see that in order that the first theorem remains valid we need the k interval to be open. Floquet's theorem is expressed finally as:

$$\psi^{E\lambda}(x) \equiv \psi_k^E(x) = e^{ikx} \phi^E(x) \quad \text{where: } \phi^E(x + a) = \phi^E(x) \quad (2.28)$$

Now we are going to reformulate equation [2.24] in terms of the fundamental solutions of eq . [2.10]:

$$T\psi^{E\lambda}(x) = \lambda \cdot \psi^{E\lambda} \longrightarrow \sum_{l=1}^2 \sum_{i=1}^2 (A_\lambda)^l \cdot M(a, E)_l^i \cdot \psi_i^E(x) = \lambda \cdot \sum_{i=1}^2 (A_\lambda)^i \cdot \psi_i^E(x) \quad (2.29)$$

Notice that the coefficients of the expansion of $\psi^{E\lambda}$ depend on λ because the fundamental solutions of a differential equation cannot depend on the eigenvalue of the translation

operator, so λ must be understood as the label of the i coefficient. Given that $\psi_j^E(x)$ are independent we obtain:

$$\sum_{l=1}^2 M(a, E)_l^i \cdot (A_\lambda)^l = \lambda \cdot (A_\lambda)^i \quad (2.30)$$

Then, we observe that $\begin{pmatrix} (A_\lambda)^1 \\ (A_\lambda)^2 \end{pmatrix}$ is an eigenvector of $M(a, E)$ with eigenvalue λ .

Let $\lambda_1, \lambda_2 \in \mathbb{C}$ be the eigenvalues of the fundamental matrix at $x=a$. Then, in some basis we have:

$$M(a, E) = \begin{pmatrix} \lambda_1 & 0 \\ 0 & \lambda_2 \end{pmatrix} \quad (2.31)$$

We can calculate the determinant and the trace of this matrix that are independent of the basis chosen:

$$\det(M(a, E)) = \lambda_1 \cdot \lambda_2 = 1 \quad \text{see eq [2.15]} \quad (2.32)$$

$$\text{tr}\{M(a, E)\} = \lambda_1 + \lambda_2 \quad (2.33)$$

From the former equation and [2.26] we have that:

$$\lambda_2 = 1/\lambda_1 = e^{-ik \cdot a} \longrightarrow \text{tr}\{M(a, E)\} = \lambda_1 + \lambda_2 = 2 \cdot \cos(k \cdot a) \quad (2.34)$$

Recall the definition of the fundamental matrix eq. [2.13], so in that basis the trace is:

$$\text{tr}\{M(a, E)\} = \psi_1^E(a) + \frac{d\psi_2^E}{dx}(a) \quad (2.35)$$

It is customary to define the following function:

$$\gamma(E) = \cos(k \cdot a) = \frac{1}{2} \left(\psi_1^E(a) + \frac{d\psi_2^E}{dx}(a) \right) \quad (2.36)$$

Due to the first theorem γ is an entire function of E because it is defined as the sum of two entire functions. This function is known once the fundamental solutions of the differential equation are obtained.

Suppose we know a solution of equation [2.36] (E_0, k_0) , by continuity of γ any E in a sufficiently small neighborhood of E_0 solves equation [2.36] for some k . Otherwise, suppose that E_0 does not solve equation [2.36] for any k , then any E in a sufficiently small neighborhood of E_0 does not solve equation [2.36]. But this is not necessarily the case for the extreme points of the interval, that is $k = \pi/a$, because γ would not be continuous at this point if this was the case contradicting the first theorem. So the domain of k is restricted to $k \in \left(-\frac{\pi}{a}, \frac{\pi}{a}\right)$, see [15]. □

In conclusion, in the one dimensional case, if the potential is periodic then the spectrum of the Hamiltonian of the system consists of the union of separate open intervals, commonly called energy bands in physics literature.

3 Theoretical background

3.1 The Born-Oppenheimer approximation

The form of the general non-relativistic Hamiltonian for a molecular cluster or a solid is:

$$\begin{aligned}
 \hat{H} &= \hat{T}_e + \hat{V}_{ee} + \hat{T}_N + \hat{V}_{NN} + \hat{V}_{eN} = \\
 &= \underbrace{\sum_{i=1}^{N_e} \frac{\hat{P}_i^2}{2m_i}}_{= \hat{T}_e, \text{ kinetic energy of the electrons}} + \underbrace{\frac{1}{2} \sum_{i=1}^{N_e} \sum_{j=1}^{N_e} \frac{e^2}{|\hat{r}_{ij}|}}_{= \hat{V}_{ee}, \text{ Coulomb interaction between the electrons}} + \underbrace{\sum_{I=1}^{N_c} \frac{\hat{P}_I^2}{2m_I}}_{= \hat{T}_N, \text{ kinetic energy of the nuclei}} + \underbrace{\sum_{I=1}^{N_c} \sum_{J=1}^{N_c} \frac{z_I z_J e^2}{|\hat{R}_{IJ}|}}_{= \hat{V}_{NN}, \text{ Coulomb interaction between nuclei}} - \underbrace{\sum_{i=1}^{N_e} \sum_{I=1}^{N_c} \frac{z_I e^2}{|\hat{R}_I - \hat{r}_i|}}_{= \hat{V}_{eN}, \text{ Coulomb interaction between nuclei and electrons}} \quad (3.1)
 \end{aligned}$$

where $z_I e$ and e are the charge of the nuclei and the electrons, respectively and Z_I is the atomic number of the I atom. There are $3N_e$ variables describing electrons, \vec{r}_i , labeled with lowercase Latin indices, and $3N_c$ variables describing cores, \vec{r}_I , labeled with uppercase Latin indices, see [8].

Without doing any approximations this Hamiltonian is very difficult to deal with. It is not only about the dimensionality of the problem, $3N_e + 3N_c$, but the coupling degrees of freedom makes the eigenstate equation unsolvable, as we just cannot solve a system of $3N_e + 3N_c$ coupled differential equations. In order to reduce the size of the problem, we can neglect the motion of the cores due to the difference of masses between nucleons and electrons ($m_I/m_e \sim 5 \cdot 10^{-4}$). This approach is known as *the Born-Oppenheimer approximation*. The kinetic energy of the nuclei term is not the only term that vanishes, but also the potential due to core-core interactions is constant, so we can ignore it in order to solve the eigenstate equation for the electrons. In conclusion, the Hamiltonian that we are going to consider from now on is:

$$\hat{H} = \sum_{i=1}^{N_e} \frac{\hat{P}_i^2}{2m_i} + \sum_{i=1}^{N_e} V_{nucl}(\hat{r}_i) + \frac{1}{2} \sum_{i=1}^{N_e} \sum_{j=1}^{N_e} \frac{e^2}{|\hat{r}_{ij}|} \quad (3.2)$$

The term that contains the information about the material is:

$$V_{nucl}(\hat{r}_i) = - \sum_{I=1}^{N_c} \frac{z_I e^2}{|\hat{R}_I - \hat{r}_i|} \quad (3.3)$$

3.2 The electron density

The particle density operator of a N -particles system is defined as, see [8]:

$$\hat{n}(\vec{r}) := \sum_{i=1}^N \delta(\vec{r} - \vec{r}_i) \quad (3.4)$$

where \vec{r}_i are the coordinates that describe each particle. The particle density operator is the analog to the charge density of points charges in classical electrodynamics. The difference is that we cannot talk about the precise position of electrons anymore but of their probability

to be found at a certain position. The expectation value of this operator for a given state, ψ , is the *particle density*:

$$n(\vec{r}) = \frac{\langle \psi | \hat{n}(\vec{r}) | \psi \rangle}{\langle \psi | \psi \rangle} = N \int \psi(\vec{r}, \vec{r}_2 \cdots \vec{r}_N) \psi^*(\vec{r}, \vec{r}_2 \cdots \vec{r}_N) d^3r_2 \cdots d^3r_N \quad (3.5)$$

where ψ is a state of the N-particle system normalized to 1.

The density is nothing but the probability to found a particle of the system at the position \vec{r} . So the normalization condition for ψ can be written as :

$$N = \int n(\vec{r}) d^3r \quad (3.6)$$

This is precisely the reason why this expectation value is called the electron density, because it is a function of the spatial coordinates that integrated over all the space give us the number of electrons.

This quantity does not seem in principle a very promising one to solve our problem but we will see that is indeed the key function. The reason for this is that the properties of a system of interacting fermions is uniquely determined by the electron density of the ground state of the system according to a celebrated theorem from 1964 by Hohenberg and Kohn, see [9].

3.3 The Hohenberg-Kohn theorem(s)

The variational principle of Quantum Mechanics is the theorem that will allow us to establish a direct relation between the density and the potential generated by the ions of the material V_{eN} , but it also provides the path to derive the so called Kohn-Sham equations. The theorem states that the expectation value of the Hamiltonian reaches a minimum at the ground state of the system, i.e:

$$\frac{\langle \psi | \hat{H} | \psi \rangle}{\langle \psi | \psi \rangle} \geq E_G \quad (3.7)$$

where E_G is the energy of the ground state.

Theorem 1. The ground state of the system is determined uniquely by its particle density.

Proof. The first step of the proof is showing that the density determines uniquely the external potential V_{ext} (\hat{V}_{eN}). Let's assume that there exist two different potentials $V_{ext}^{(1)}$ and $V_{ext}^{(2)}$, whose difference is not just a constant, that lead to the same density $n(\vec{r})$, and that admit the decomposition:

$$V_{ext}^{(i)} = \sum_{j=1}^N v_{ext}^{(i)} \quad (3.8)$$

Therefore there are two different Hamiltonian \hat{H}_1 and \hat{H}_2 . Consequently, the ground states of these Hamiltonians are different, namely $|\psi_1\rangle$ and $|\psi_2\rangle$ with associated energies $E^{(1)}$ and $E^{(2)}$, respectively. Taking into account that $|\psi_2\rangle$ is not the ground state of \hat{H}_1 , it follows from [6] that:

$$E^{(1)} = \langle \psi_1 | \hat{H}_1 | \psi_1 \rangle < \langle \psi_2 | \hat{H}_1 | \psi_2 \rangle \quad (3.9)$$

The second term can be written as:

$$\begin{aligned}\langle \psi_2 | \hat{H}_1 | \psi_2 \rangle &= \langle \psi_2 | \hat{H}_2 | \psi_2 \rangle + \langle \psi_2 | \hat{H}_1 - \hat{H}_2 | \psi_2 \rangle = \\ &= E^{(2)} + \int \left(v_{ext}^{(1)}(\vec{r}) - v_{ext}^{(2)}(\vec{r}) \right) n(\vec{r}) d^3r > E^{(1)}\end{aligned}\quad (3.10)$$

Swapping the indices (1) and (2) we get the inequality:

$$E^{(2)} < E^{(1)} + \int \left(v_{ext}^{(2)}(\vec{r}) - v_{ext}^{(1)}(\vec{r}) \right) n(\vec{r}) d^3r \quad (3.11)$$

Adding up both sides of the inequalities we get:

$$E^{(1)} + E^{(2)} < E^{(1)} + E^{(2)} \quad \# \quad (3.12)$$

Thus, there are not two different external potentials leading to the same particle density, i.e, there exist a one to one relation between the external potential and the particle density:

$$n(\vec{r}) \iff V_{ext}(\vec{r}) \quad (3.13)$$

This result allows us to write $V_{ext} = V_{ext}[n]$, and therefore, the full Hamiltonian is determined by the density, as well as the ground state of the system, $|\psi\rangle = |\psi[n]\rangle$.

Theorem 2. For any external potential V_{ext} , an energy functional:

$$E^{(HK)}[n] = F_{(HK)} + \int v_{ext}(\vec{r}) n(\vec{r}) d^3r \quad (3.14)$$

can be defined, with $F_{(HK)}[n]$ a universal functional, independent of the external potential. For a particular choice of the potential v_{ext} , the energy functional $E^{(HK)}$ has a minimum when $n(\vec{r})$ is the ground state density $n_0(\vec{r})$, and $E^{(HK)}[n_0(\vec{r})]$ is the ground state energy.

Proof. Let $C_{(n)}$ be the set of all the wave functions with density n , see [11]:

$$C_{(n)} := \left\{ \psi \in \mathcal{H} : n = N \int \psi^*(\vec{r}) \psi(\vec{r}) d^3r \right\} \quad (3.15)$$

Then, from the variational principles of quantum mechanics, it follows:

$$E_G \leq \min_{\psi \in \mathcal{H}} [\langle \psi | \hat{H} | \psi \rangle] = \min_n \left[\min_{\psi \in C_{(n)}} \langle \psi | \hat{H} | \psi \rangle \right] = \min_n \left(E^{(HK)}[n] \right) \quad (3.16)$$

where $E^{(HK)}[n]$ is:

$$E^{(HK)}[n(\vec{r})] := \min_{\psi \in C_{(n)}} \left[\langle \psi[n] | \underbrace{\hat{T} + \hat{V}_{ee} + \hat{V}_{ext}}_{\hat{H}} | \psi[n] \rangle \right] = \min_n \left[\underbrace{T[n] + V_{ee}[n]}_{F^{(HK)}[n]} + \int v_{ext}(\vec{r}) \cdot n(\vec{r}) d^3r \right] \quad (3.17)$$

where $F^{(HK)}[n]$ is a universal functional in the sense that it does not depend on v_{ext} . Therefore, it is independent of the material as long as we state beforehand that v_{ext} is the only term that contains the information about the underlying crystalline structure. Thus, if n_0 is the density that minimized 3.17, then $E^{(HK)}[n_0] = E_G$, i.e. the ground state energy of the system.

3.4 The Kohn-Sham equations

There is no straightforward method to calculate the universal functional $F^{(HK)}[n]$ because there is no analytic expression for the one to one relation between n and V_{ext} , so there is no evident way to minimize the last functional through the density. In 1965, Kohn-Sham [12] proposed a practical approach to this problem: to recast the many-body interacting problem using an auxiliary non interacting system. They proposed as an ansatz that, for every ground state density $n_G(\vec{r})$ of an interacting electron system, there exists a non-interacting system with the same ground state density.

For a non-interacting system, with single-particle eigenstates ϕ_i , the density can be decomposed as:

$$n(\vec{r}) = \sum_{i=1}^N \phi_i(\vec{r}) \cdot \phi_i^*(\vec{r}) \quad (3.18)$$

Using the second quantization formalism it can be shown that the effective potential according to first order perturbation theory is the interaction between two charged densities, which coincides with the Hartree potential:

$$V_H[n] = \frac{1}{2} \int n(\vec{r}) \left(\frac{e^2}{|\vec{r} - \vec{r}'|} \right) n(\vec{r}') d^3r d^3r' \quad (3.19)$$

So, it is convenient to explicitly show this term in the general formulation.

The kinetic energy of the non-interacting system which will allow us to interpret the equation obtained by means of the variational principle, is:

$$T_o[n] = \sum_{i=1}^N \langle \phi_i | \hat{T} | \phi_i \rangle = - \left(\frac{\hbar^2}{2m} \right) \sum_{i=1}^N \int (\Delta \phi_i) \phi_i^* d^3r \quad (3.20)$$

Then, the energy functional is written as:

$$\begin{aligned} E^{(HK)} &= T[n] + V_{ee}[n] + \int V_{ext}(\vec{r}) n(\vec{r}) d^3r = \\ &= T_o[n] + V_H[n] + \int V_{ext}(\vec{r}) n(\vec{r}) d^3r + E_{XC}[n] \end{aligned} \quad (3.21)$$

where the last term is the so called exchange and correlation energy, namely:

$$E_{xc}[n] = (T[n] - T_o[n]) + (V_{ee}[n] - V_H[n]) \quad (3.22)$$

Notice that, up to now, no approximation has been made.

The advantage of writing $E^{(HK)}[n]$ as in 3.21 is that, using the variational principle, we can easily derive the Kohn-Sham equations (see appendix):

$$\left[- \left(\frac{\hbar^2}{2m} \right) \Delta + V_{eff}(\vec{r})[n] \right] \phi_i(\vec{r}) = \varepsilon_i \phi_i(\vec{r}) \quad (3.23)$$

with:

$$\begin{aligned} V_{eff}(\vec{r}) &= V_H'(\vec{r}) + V_{nucl}(\vec{r}) + V_{xc}(\vec{r})[n] = \\ &= \underbrace{\frac{1}{2} \int n(\vec{r}) \left(\frac{e^2}{|\vec{r} - \vec{r}'|} \right) d^3r'}_{V_H'(\vec{r})} \underbrace{- \sum_{I=1}^{N_c} \frac{Z_I e^2}{|\hat{R}_I - \hat{r}|}}_{V_{nucl}(\vec{r})} + \underbrace{\frac{\delta E_{xc}}{\delta n}}_{V_{xc}(\vec{r})[n]} \end{aligned} \quad (3.24)$$

Then, the ground state of the system is shown to be:

$$E_G = \sum_{j=1}^N \varepsilon_j + E_{xc} - \int V_{xc}(\vec{r}) n(\vec{r}) d^3r - \frac{e^2}{2} \int \frac{n(\vec{r}) \cdot n(\vec{r}')}{|\vec{r} - \vec{r}'|} d^3r d^3r' \quad (3.25)$$

The Kohn-Sham equations are the analog of the Schrödinger equations for independent particles in an effective field V_{eff} . The main difficulty is the exchange and correlation term V_{xc} because it is the only unknown in this equation: just as an example, the expectation value of the kinetic energy of the interacting system is unknown till we solve the problem. Notice that the former development admit many generalization as for an spin-polarized system, multi-component system and even ensemble from statics physics! From now on, we will discuss the different methods that are used in order to overcome all those difficulties.

3.5 Approximation methods

3.5.1 Local density approximation (LDA) and generalized gradient approximation (GGA)

All the formalism described before makes no sense unless we are able to develop some approximating expression for the exchange and correlation functional E_{xc} . One of the most usual approximations is the so called *Local Density Approximation* (LDA), in which we assume that the density changes slowly and that the functional takes the form:

$$E_{xc}^{(LDA)}[n(\vec{r})] = \int \varepsilon_{xc}(\vec{r}) n(\vec{r}) d^3r \quad (3.26)$$

where ε_{xc} is the many-body energy per electron of an uniform gas of interacting electrons with density $n(\vec{r})$. There exist Monte Carlo calculations that provide an analytic expression of ε for an unpolarized homogeneous electron gas, see [8]. In this approximation, the exchange and correlation potential takes the form:

$$V_{xc}(\vec{r})[n(\vec{r})] = \varepsilon_{xc}(\vec{r}) + n(\vec{r}) \frac{d\varepsilon(n(\vec{r}))}{dn(\vec{r})} \quad (3.27)$$

and the ground state of the system within this approximation is:

$$E_G = \sum_{j=1}^N \varepsilon_j - \int n(\vec{r}) \frac{d\varepsilon(n(\vec{r}))}{dn(\vec{r})} d^3r - \frac{e^2}{2} \int \frac{n(\vec{r}) \cdot n(\vec{r}')}{|\vec{r} - \vec{r}'|} d^3r d^3r' \quad (3.28)$$

Another level of the approximation is to assuming that ε_{xc} depends also on the gradient of the density, rather than only on the density:

$$E_{xc}^{(GGA)}[n(\vec{r})] = \int \varepsilon_{xc}(n(\vec{r}), \vec{\nabla} n(\vec{r})) n(\vec{r}) d^3r \quad (3.29)$$

which is the approximation we will use in order to perform the calculations for diamond and graphite. This approximation is known as the *Generalized Gradient Approximation* (GGA).

Even though, we will need further approximations in order to make the calculations of the solutions of the Kohn-Sham equations computationally accessible, such as using a plane wave basis orthogonalized to core states, or to use different potential in the inner core region that reproduce the outer region states.

3.5.2 The plane waves (PW) and the orthogonal plane waves (OPW) method

Plane waves are a suitable basis set of functions because they incorporate in a matricial way the PBC of the system, that is, the kinetic energy operator is diagonal in this basis and the matrix element of the potential involve its Fourier transform. For a given wave vector $\vec{k} \in \mathbf{FBZ}$ we define the set:

$$\langle \vec{r} | \vec{k} + \vec{G}_i \rangle = W_{\vec{k}_i}(\vec{r}) = \frac{1}{\sqrt{\Omega}} e^{i\vec{k}_i \cdot \vec{r}} \quad (3.30)$$

with $\vec{k}_i = \vec{k} + \vec{G}_i$, $\vec{G}_i \in \mathbf{R}^*$ and Ω is the volume of region where the plane wave is orthogonalized. The wave vectors are chosen such that if $i > j$ the kinetic energy of the plane wave associated with \vec{G}_i is greater than the associated with \vec{G}_j .

The potential that is considered is the effective potential of the Kohn-Sham equations using Rydberg atomic units ²:

$$V(\vec{r}) = \frac{1}{2} \int n(\vec{r}') \left(\frac{e^2}{|\vec{r} - \vec{r}'|} \right) d^3 r' - \sum_{I=1}^{N_c} \frac{z_I e^2}{|\hat{R}_I - \hat{r}|} + V_{xc}(\vec{r}) \quad (3.31)$$

The matrix elements of the Hamiltonian in this basis set:

$$\begin{aligned} \langle \vec{k} + \vec{G}_i | \hat{H} | \vec{k} + \vec{G}_j \rangle &= \langle \vec{k} + \vec{G}_i | -\Delta | \vec{k} + \vec{G}_j \rangle + \int_{\Omega} W_{\vec{k}_i}^*(\vec{r}) V(\vec{r}) W_{\vec{k}_j}(\vec{r}) d^3 r = \\ &= k_j^2 \delta_{ij} + \underbrace{\frac{1}{\Omega} \int_{\Omega} V(\vec{r}) \cdot e^{-i(\vec{G}_i - \vec{G}_j) \cdot \vec{r}} d^3 r}_{v(\vec{G}_i - \vec{G}_j)} = k_j^2 \delta_{ij} + v(\vec{G}_i - \vec{G}_j) \end{aligned} \quad (3.32)$$

The matrix elements of the Hamiltonian are nothing but the Fourier transform of the effective potential for the auxiliary system plus a contribution coming from the kinetic energy operator which is diagonal in this representation (in practice, it can be convenient to consider a non-local potential $\langle \vec{r} | v | \vec{r}' \rangle = v(\vec{r}, \vec{r}')$, but in these notes we will consider for the sake of simplicity the case of a local potential $\langle \vec{r} | v | \vec{r}' \rangle = v(\vec{r}, \vec{r}') \delta(\vec{r} - \vec{r}')$)

The plane waves basis previously defined allows us to expand any wave function $\psi_{\vec{k}}(\vec{r})$ with a fixed wave vector $\vec{k} \in \mathbf{FBZ}$ as ³:

$$\psi_{\vec{k}}(\vec{r}) = e^{i\vec{k} \cdot \vec{r}} \underbrace{\left[\sum_{i=0}^{\infty} c_i(\vec{k}) \cdot \frac{e^{i\vec{G}_i \cdot \vec{r}}}{\sqrt{\Omega}} \right]}_{u_{\vec{k}}(\vec{r})} = \sum_{i=0}^{\infty} c_i(\vec{k}) \cdot W_{\vec{k}_i}(\vec{r}) \quad (3.33)$$

The ground state energy of the system for a given state $\psi_{\vec{k}}(\vec{r})$ can be obtained by means of the variational principle of Quantum Mechanics (eq. 3.7) :

$$\begin{aligned} \langle \psi_{\vec{k}} | \hat{H} | \psi_{\vec{k}} \rangle &= \sum_{i=0}^{\infty} \sum_{j=0}^{\infty} c_i^*(\vec{k}) c_j(\vec{k}) \langle W_{\vec{k}_i}(\vec{r}) | \hat{H} | W_{\vec{k}_j}(\vec{r}) \rangle = \sum_{i=0}^{\infty} \sum_{j=0}^{\infty} c_i^*(\vec{k}) c_j(\vec{k}) [k_j^2 \delta_{ij} + v(\vec{G}_i - \vec{G}_j)] = \\ &= \sum_{i=0}^{\infty} c_i^*(\vec{k}) \left\{ \sum_{j=0}^{\infty} c_j(\vec{k}) [k_j^2 \delta_{ij} + v(\vec{G}_i - \vec{G}_j)] \right\} = E \end{aligned} \quad (3.34)$$

²see Appendix A-1: Atomic units.

³See Bloch's theorem for the multidimensional case A.2.

Introducing E into the summation:

$$\langle \psi_{\vec{k}} | \hat{H} | \psi_{\vec{k}} \rangle = \sum_{i=0}^{\infty} c_i^*(\vec{k}) \left\{ \sum_{j=0}^{\infty} c_j(\vec{k}) \left[(k_j^2 - E) \delta_{ij} + v(\vec{G}_i - \vec{G}_j) \right] \right\} = 0 \quad (3.35)$$

The term between brackets must be zero because the coefficients of the expansion are independent:

$$\sum_{j=0}^{\infty} c_j(\vec{k}) \left[(k_j^2 - E) \delta_{ij} + v(\vec{G}_i - \vec{G}_j) \right] = 0 \quad (3.36)$$

The last equation is a homogeneous linear system. In order to have a non-trivial solution the determinant of the associated matrix must be zero:

$$\det \left((k_j^2 - E) \delta_{ij} + v(\vec{G}_i - \vec{G}_j) \right) = 0 \quad (3.37)$$

So far the expansion of the bloch's functions has not been truncated but one needs to define a cut-off energy E_c . In order that plane waves expansion [3.33] converge to $\psi_{\vec{k}}(\vec{r})$, the coefficients of the expansion ($c_{\vec{k}}$) must decrease when $\|\vec{G}_i\|$ increase. In the literature it is usual to define the cut off energy based on the kinetic energy of the plane waves:

$$E_c \geq \frac{\hbar^2}{2m_i} \cdot \|\vec{k} + \vec{G}_i\| \quad (3.38)$$

The problem of expanding crystal states in a plane wave basis is the huge number of coefficients needed to reproduce them. The physical origin of this problem comes from the divergence of the Coulomb's potential at the core positions producing rapid oscillations in the wavefunctions.

The number of coefficients needed can be reduced if we consider that the cores states ($\psi_n^{\text{core}}(\vec{r})$) are already known, that is, the eigenvalue problem for those states are solved:

$$\hat{H} \psi_n^{\text{core}}(\vec{r}) = E_n^{\text{core}} \cdot \psi_n^{\text{core}}(\vec{r}) \quad n = 1, 2, \dots, n_c \quad (3.39)$$

These states do not satisfy Floquet's theorem, but we can define the so called **Bloch's sum** for each core state:

$$\Phi_{n,\vec{k}}^{\text{core}}(\vec{r}) = \frac{1}{\sqrt{N}} \sum_{\vec{R} \in \mathbf{R}} e^{i\vec{k} \cdot \vec{R}} \cdot \psi_n^{\text{core}}(\vec{r} - \vec{R}) \quad (3.40)$$

Notice that Bloch's sum satisfies:

$$\Phi_{n,\vec{k}}^{\text{core}}(\vec{r} + \vec{R}') = e^{i\vec{k} \cdot \vec{R}'} \cdot \Phi_{n,\vec{k}}^{\text{core}}(\vec{r}) \quad \vec{R}' \in \mathbf{R} \quad (3.41)$$

In fact, Bloch's sum have the same energy that the associated core state due to the translational invariance of the system, i.e., $[\hat{H}, \hat{T}_{-\vec{R}}] = 0$:

$$\begin{aligned} \hat{H} \Phi_{n,\vec{k}}^{\text{core}}(\vec{r}) &= \frac{1}{\sqrt{N}} \sum_{\vec{R} \in \mathbf{R}} e^{i\vec{k} \cdot \vec{R}} \cdot \hat{H} \psi_n^{\text{core}}(\vec{r} - \vec{R}) = \frac{1}{\sqrt{N}} \sum_{\vec{R} \in \mathbf{R}} e^{i\vec{k} \cdot \vec{R}} \cdot \hat{H} \hat{T}_{-\vec{R}} \psi_n^{\text{core}}(\vec{r}) = \\ &= \frac{1}{\sqrt{N}} \sum_{\vec{R} \in \mathbf{R}} e^{i\vec{k} \cdot \vec{R}} \cdot \hat{T}_{-\vec{R}} \hat{H} \psi_n^{\text{core}}(\vec{r}) = \frac{1}{\sqrt{N}} \sum_{\vec{R} \in \mathbf{R}} e^{i\vec{k} \cdot \vec{R}} \cdot \hat{T}_{-\vec{R}} E_n^{\text{core}} \psi_n^{\text{core}}(\vec{r}) = E_n^{\text{core}} \cdot \Phi_{n,\vec{k}}^{\text{core}}(\vec{r}) \end{aligned} \quad (3.42)$$

The idea is to construct the secular equation [3.37] in such a way that only provide information about the more energetic states, i.e, the outer states ψ_i^{outer} (valence and conducting states). We define a set of functions orthogonal to the Bloch's sum associated to the core states as:

$$W_{\vec{k}_i}^\perp(\vec{r}) = W_{\vec{k}_i}(\vec{r}) - \sum_{n=1}^{n_c} \langle \Phi_{n,\vec{k}}^{\text{core}} | W_{\vec{k}_i} \rangle \cdot \Phi_{n,\vec{k}}^{\text{core}}(\vec{r}) \quad (3.43)$$

We can span any outer state to $\Phi_{n,\vec{k}}^{\text{core}}$ in this set as:

$$\psi_i^{\text{outer}}(\vec{r}) = \sum_{j=1}^{\infty} c_{ij} \cdot W_{\vec{k}_i}^\perp(\vec{r}) \quad (3.44)$$

From the same procedure that leads to eq. [3.37] it follows:

$$\det \left(\langle W_{\vec{k}_i}^\perp | \hat{H} | W_{\vec{k}_j}^\perp \rangle - E \langle W_{\vec{k}_i}^\perp | W_{\vec{k}_j}^\perp \rangle \right) = 0 \quad (3.45)$$

Now we will express the matrix element of the last equation in terms of the matrix element in the plane waves basis:

$$\begin{aligned} \bullet \langle W_{\vec{k}_i}^\perp | \hat{H} | W_{\vec{k}_j}^\perp \rangle &= \langle W_{\vec{k}_i} | \hat{H} | W_{\vec{k}_j} \rangle - 2 \cdot \langle W_{\vec{k}_i} | \left[\sum_{n=1}^{n_c} E_n^{\text{core}} \cdot | \Phi_{n,\vec{k}}^{\text{core}} \rangle \langle \Phi_{n,\vec{k}}^{\text{core}} | \right] | W_{\vec{k}_j} \rangle - \\ &+ \langle W_{\vec{k}_i} | \left[\sum_{n=1}^{n_c} \sum_{l=1}^{n_c} E_l^{\text{core}} | \Phi_{n,\vec{k}}^{\text{core}} \rangle \langle \Phi_{n,\vec{k}}^{\text{core}} | \Phi_{l,\vec{k}}^{\text{core}} \rangle \langle \Phi_{l,\vec{k}}^{\text{core}} | \right] | W_{\vec{k}_j} \rangle = \\ &= \langle W_{\vec{k}_i} | \hat{H} | W_{\vec{k}_j} \rangle - \langle W_{\vec{k}_i} | \left[\sum_{n=1}^{n_c} E_n^{\text{core}} \cdot | \Phi_{n,\vec{k}}^{\text{core}} \rangle \langle \Phi_{n,\vec{k}}^{\text{core}} | \right] | W_{\vec{k}_j} \rangle \end{aligned} \quad (3.46)$$

$$\begin{aligned} \bullet - E \langle W_{\vec{k}_i}^\perp | W_{\vec{k}_j}^\perp \rangle &= \langle W_{\vec{k}_i} | - E \mathbf{1} | W_{\vec{k}_j} \rangle + 2 \cdot \langle W_{\vec{k}_i} | \left[\sum_{n=1}^{n_c} E \cdot | \Phi_{n,\vec{k}}^{\text{core}} \rangle \langle \Phi_{n,\vec{k}}^{\text{core}} | \right] | W_{\vec{k}_j} \rangle - \\ &- \langle W_{\vec{k}_i} | \left[\sum_{n=1}^{n_c} \sum_{l=1}^{n_c} E | \Phi_{n,\vec{k}}^{\text{core}} \rangle \langle \Phi_{n,\vec{k}}^{\text{core}} | \Phi_{l,\vec{k}}^{\text{core}} \rangle \langle \Phi_{l,\vec{k}}^{\text{core}} | \right] | W_{\vec{k}_j} \rangle = \\ &= \langle W_{\vec{k}_i} | - E \mathbf{1} | W_{\vec{k}_j} \rangle + \langle W_{\vec{k}_i} | \left[\sum_{n=1}^{n_c} E \cdot | \Phi_{n,\vec{k}}^{\text{core}} \rangle \langle \Phi_{n,\vec{k}}^{\text{core}} | \right] | W_{\vec{k}_j} \rangle \end{aligned} \quad (3.47)$$

Taken into account the last two equations, [3.45] can be written as:

$$\begin{aligned} \det \left(\langle W_{\vec{k}_i} | \left[\hat{H} - E \mathbf{1} + \sum_{i=1}^{n_c} (E - E_n^{\text{core}}) | \Phi_{n,\vec{k}}^{\text{core}} \rangle \langle \Phi_{n,\vec{k}}^{\text{core}} | \right] | W_{\vec{k}_j} \rangle \right) &= \\ &= \det \left(\langle W_{\vec{k}_i} | \hat{H} + \hat{V}^{(\text{rep})} | W_{\vec{k}_j} \rangle - E \cdot \delta_{ij} \right) = 0 \end{aligned} \quad (3.48)$$

with :

$$\hat{V}^{(\text{rep})} = \sum_{n=1}^{n_c} (E - E_n^{\text{core}}) | \Phi_{n,\vec{k}}^{\text{core}} \rangle \langle \Phi_{n,\vec{k}}^{\text{core}} | \quad \text{with } E > E_n^{\text{core}} \quad (3.49)$$

This operator is energy dependent and non-local and can be interpreted as a repulsive potential produced by core states.

3.5.3 The pseudopotential method

In the last section the non-local repulsive potential $V^{(rep)}$ that arises from the orthogonal character of the outer states with respect to the inner states somehow reduces the interactions that feel the valence electrons. The problem that led to introduce such an effective Hamiltonian was the huge number needed in plane wave expansion in order to describe accurately the valence wave function in the inner core region. The goal behind the pseudopotential method is to reproduce the same effect by taking into account that in the core region the potential is softer than in the outer region. The natural question is what prescription shall we impose on the pseudopotential to reproduce such effect? As long as we are only interested in getting rid of the oscillating part of the valence wave function, the non-oscillating part must remain the same. For that purpose it is usual to define a cut-off radius (r_c) such that:

$$\psi^{pseudo}(\vec{r}) = \begin{cases} \psi^{nodeless}(\vec{r}) & \text{if } r < r_c \\ \psi^{real}(\vec{r}) & \text{if } r > r_c \end{cases} \quad (3.50)$$

where $\psi^{nodeless}$ is the solution obtained by solving the Schrodinger equation by replacing the all-electron interaction with the pseudopotential and ψ^{real} is the solution without such replacement. This conditions suggest a very interesting approach [10]: to construct the pseudopotential by solving the inverse problem, i.e. given a convenient nodeless form for the pseudo wave function, like [3.50], found the pseudopotential such that:

$$[-\Delta + V^{(pseudo)}]\psi_n^{pseudo}(\vec{r}) = \epsilon_n \cdot \psi_n^{pseudo}(\vec{r}) \quad (3.51)$$

where ϵ_n are the original eigenvalues of the original Hamiltonian. The pseudo wave function can be separated into radial and angular parts: $R_{nl}(r)$, $Y_l^m(\theta, \psi)$. The radial Schrödinger equation for the radial part of the pseudo wave function is:

$$\left[\frac{d^2}{dr^2} + \frac{l(l+1)}{2r^2} + V^{(pseudo)}(r) \right] r R_{nl}(r) = \epsilon_n r R_{nl}(r) \quad (3.52)$$

with continuity of the radial wave function and its derivative:

$$R_{nl}(r) = \begin{cases} R_{nl}^{pseudo}(r) & \text{if } r < r_{c,l} \\ R_{nl}^{real}(r) & \text{if } r > r_{c,l} \end{cases} \quad (3.53)$$

It can be shown that the solution of this equation is uniquely determined by the value of the radial wave function and its derivative at $r_{c,l}$. This conditions can be written as:

$$\left. \frac{d}{dr} \log(R_{nl}^{(real)}(r)) \right|_{r_{c,l}} = \frac{1}{R_{nl}^{(pseudo)}(r_c)} \left. \frac{dR_{nl}^{(pseudo)}(r)}{dr} \right|_{r_{c,l}} \quad (3.54)$$

A further request is needed in order that the density in the core is correctly normalized, this is:

$$\int_0^{r_{c,l}} r^2 [R_{nl}^{(real)}(r)]^2 dr = \int_0^{r_{c,l}} r^2 [R_{nl}^{(pseudo)}(r)]^2 dr \quad (3.55)$$

This is the so called *norm-conservation condition*.

In order to solve for $V^{(pseudo)}(r)$ in eq. [3.51] we must solve the radial equation for a *reference configuration* using the effective potential [3.31] to obtain the radial wave function:

$$V^{(pseudo)}(r) = \epsilon_n - \frac{l(l+1)}{2r^2} + \frac{1}{2r R_{nl}^{(pseudo)}(r)} \frac{d^2}{dr^2} [r R_{nl}^{(pseudo)}(r)] \quad (3.56)$$

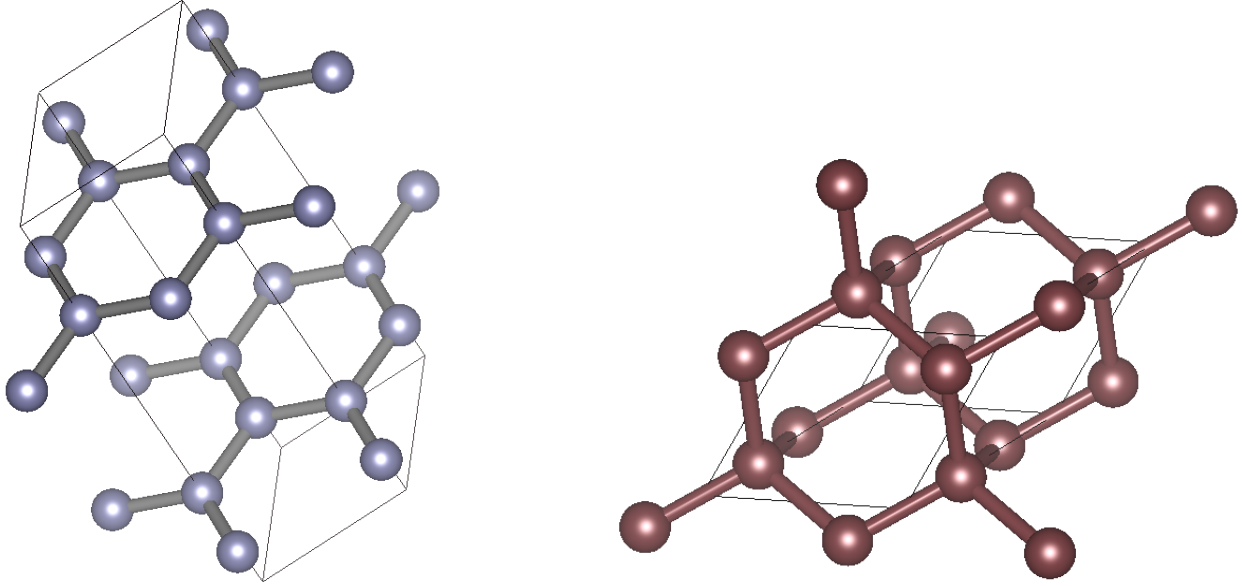


Figure 2: Conventional cells of graphite and diamond.

4 Ab initio calculations for selected materials

4.1 Introduction

In the previous chapters we summaries the general density functional framework for the study of solids in the hope that this approach would make affordable the computation of the solution of the N-body problem. The density plays a fundamental role in this scheme, as it allows us to transform the N-body problem into N one-body problems. Then, we discussed how the rapid oscillation of the wave function, due to the divergence of the Coulomb's potential at the core positions, needs too many plane waves for its expansion, leading to first the concept of orthogonal plane wave expansion (OPW) and later, to the concept of pseudopotential. The goal of this chapter is to make use of all these methods, and others that we do not explicitly explain because it is out of the scope of this work, to study diamond and graphite, the two natural forms of carbon (see figure [3] generated using the free software package **VESTA** [3], which is dedicated to the visualization for electronic and structural analysis). These materials were chosen because they are the best examples of how the structure of a system has a huge impact on its properties : for instance, diamond is known as the hardest material, but this is not the case of the graphite, even when both are made up of the same chemical element.

In this chapter we will go through the entire process of the simulations, putting special emphasis on their generation procedure and comparing the results with the experiments, when this is possible.

4.2 Methodology

In order to perform the calculation we used the **Viena Ab initio Simulation Package** (VASP), which implements the DFT methodology explained in the previous sections in a scheme of pseudopotentials and a basis of plane waves. First, we are going to explain how to configure a general simulation and what is the configuration chosen in our case.

We have to differentiate four different input files:

1. **POSCAR:** In this file we introduce the structure of the material we are interested in, i.e. we introduce the coordinates of the lattice generators [2.1] in a three by three matrix and the position of the atoms with respect to this basis. If we were interested in a bidimensional material, we would have to simulate it by enlarging the third dimension, so that we get layers sufficiently separated so that the interaction between them is negligible.
2. **POTCAR:** This file contains the pseudopotential for each atomic species of the material, as it appears in the official site of VASP [2]. There are different methods designed to calculate the pseudopotential, and so there are different options to choose for each atomic species.
3. **KPOINTS:** This file contains the grid for the Brillouin zone integration, or in general, for solving the Kohn-Sham equations. There are two main options: to introduce the spacing of the mesh and choose a method to create it automatically, or to introduce it manually. The latter is very convenient to calculate the band structure of the material along high symmetry directions once a self-consistent calculation has been performed and we have the ground state charge density.
4. **INCAR:** This file contains the parameters of the simulation, such as the method used to integrate over the mesh declared in the KPOINTS file, the energy cut-off in the plane wave expansion, the treatment of the Fermi surface, and what type of calculations one is going to perform (self-consistent, atomic relaxation previous atomic relaxation calculation of stress and forces, etc). The specific parameters will be discussed along this section because each one of them needs to be explained in the proper context.

The structure of the material is known from X-ray diffraction experiments, i.e. the position of the atoms and the symmetry of the lattice, see [14] to see how this is done. This is the only information, together with the atomic species involved, that we know about the material, which is the main reason why this kind of simulations are called **ab initio**, or **from first principles**, as the knowledge of the underlying crystal structure of the material is enough to compute all of its properties. We have to study the convergence of the energy with the cut-off energy [3.38] and the number of points chosen on the Brillouin zone (k-points for short from hereafter) in order to set its optimal values for the later calculations. In order to test the convergence of the energy with the cut-off energy we have to fix the configuration and the k-points and check whether the difference between the energies obtained changes from one particular cut-off energy to another or not. The same argument works for studying the convergence of the energy with the k-points. The set up of the KPOINTS file is more complicated. We need to choose the spacing of the grid of the Brillouin zone on each direction. For instance, in the case of the diamond we choose an uniform spacing on the three directions, but this is not the case on graphite. In order to try to cover the Brillouin zone uniformly, we need to take into account that the cell is hexagonal, and that there are two lattice parameters, a and c , where a is the lattice parameters of the hexagonal lattice in the same layer and c is the distance between layers. We choose the same spacing in two directions and the third part of the former spacing in the third direction. Both tests can be seen in figure [3]. In this situation, we choose as cut-off energy 520 eV in both cases. As mentioned above, for diamond we choose a uniform grid of $8 \times 8 \times 8$ and for the graphite $24 \times 24 \times 8$. This means that the method that generates the grid of the Brillouin zone will take, for example, 24 points along the x and y directions and 8 along the z direction (in the reciprocal space).

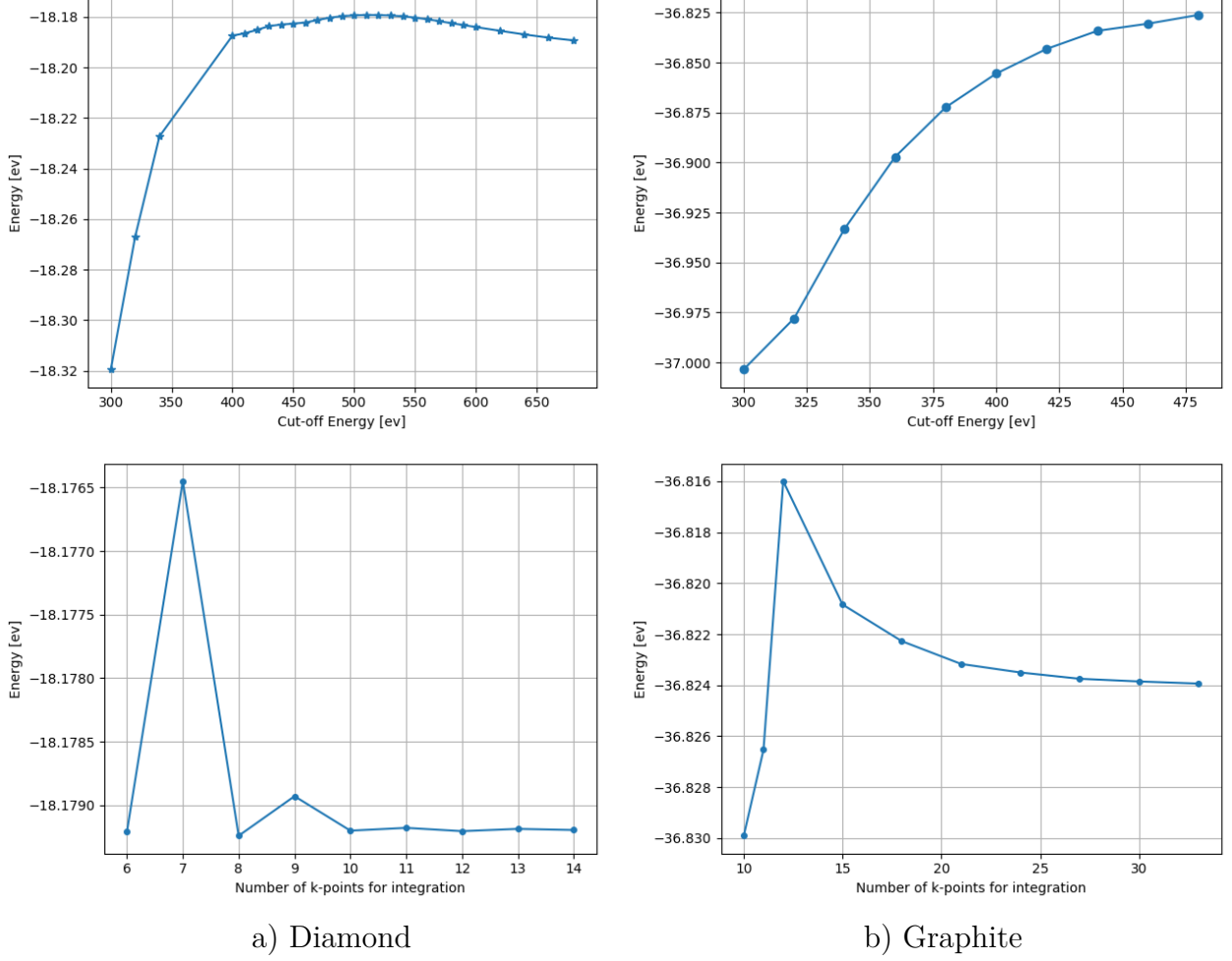


Figure 3: First row: test of convergence in the cut-off energy. Second row: test of convergence of the energy in the number of k-points.

4.3 Details of the calculations

The calculations are done using a **self-consistent method**. The method starts using a trial density function $n_{\text{trial}}(\vec{r})$ and solves Kohn-Sham equations [3.23], or a generalized version of them. From the solutions a new density can be computed, $n_{\text{out}}(\vec{r})$. This method is called self-consistent because if $n_{\text{trial}}(\vec{r}) - n_{\text{out}}(\vec{r}) > \varepsilon$ for some fixed threshold ε , then the Kohn-Sham equations are solved again but using a modified density $n(\vec{r})$, constructed from n_{trial} and n_{out} as the new trial density. This process stops when the difference between the trial density and the one obtained by solving the equations is less than ε .

Once the solution of the self-consistent method is obtained, the forces between the atoms must be checked. The forces on the i -th atom are computed as the minus the gradient of the energy with respect to the atomic positions:

$$\vec{F}_i = -\vec{\nabla}_{\vec{r}_i} E \quad (4.1)$$

We have to take into account that the whole system must be in its ground state, which includes the cores, but with the Born-Oppenheimer approximation we get rid of the dynamics of all the ions, and they are only seen by the electrons because of the field they produce through the pseudopotential. Then, we must also find the ground state for the structure by optimizing

the lattice position of the ions so that the forces on them are ideally become zero. The same argument works for the stress tensor, whose components are defined as the derivative of the energy with respect to the strain tensor, but with the difference that we now allow a diagonal stress tensor, which means that the pressure that the material feels is hydrostatic. Then, once we move an ion or deform the cell, we must start again the self-consistent electronic method in order to obtain the correct density for the new configuration. We will say that the structure is *relaxed* if the the forces acting on each atom are zero and the stress tensor is diagonal. Sometimes we may not want the system to relax, and in those cases we just need to indicate it in the INCAR file.

4.4 Results and analysis

In the following discussion we are going to present the results obtained using the optimal values of the cut-off energy and the k-points introduced in the previous section. In order to achieve better clarity in our exposition, we will structure these results in three main sections: in the first one we include the direct results of the simulations and the appropriate numerical fit to a state equation (EOS), as well as discussing the evolution of the lattice parameters and obtaining the bulk modulus. After this, we will explain the procedure followed in order to compute the energy bands, and finally a brief introduction to the *electronic localization function* (ELF) will be made.

4.4.1 Equations of state

The main aim of this section is describing the computational procedure followed to calculate, analyze and process the raw output data produced by the simulations. This procedure starts by introducing the numerical information that corresponds to the volume of each primitive cell of the material, which allows the program to automatically adjust the lattice parameters to the input volume. Once the software has finished this process, we carry out an indexed search in the OUTCAR output file using the Linux *grep* command, in order to extract the numerical values of pressure and energy. As we also need to eliminate the unnecessary information from the output string, and this process needs to be repeated for every single volume, we resort to the creation of a *Python* program that will automate the parsing and create a file ready to be used for graphical representations.

Up to this point, the influence of residual dipole-dipole interaction between atoms, which is called Van der Waals interaction, in the studied materials has not been taken into account, but it needs to be introduced if we want to explain the stability of graphite, as in its absence no visible energy minimum can be detected in the energy-volume curve. The necessary computational processes for the inclusion of this interaction in the calculations is already implemented in the *VASP* routine, we only need to activate a flag in the INCAR file, and repeat the previous calculations. The previous absence of an energy minimum for graphite is now resolved, as can be seen in figure 4, where a clear minimum can be observed. Based on this graph we can also conclude that the only effect of the Van der Waals interaction on diamond is a shift on the energy values, that we removed by changing the energy reference.

The following graph also shows various numerical fits to the calculated data, which is our next step in the analysis of the simulation results. These fits have been computed using the Birch-Murnaghan equation with four free parameters, B_0 , B'_0 , V_0 and E_0 , whose optimal

values in a least-squares approach can be found for each data set:

$$E(V) = E_0 + \frac{9V_0B_0}{16} \left\{ \left[\left(\frac{V_0}{V} \right)^{\frac{2}{3}} - 1 \right]^3 B'_0 + \left[\left(\frac{V_0}{V} \right)^{\frac{2}{3}} - 1 \right]^2 \right\} \quad (4.2)$$

where B_0 denotes the bulk modulus and the subindex refers to the equilibrium volume (V_0):

$$B_0 = -V_0 \left(\frac{\partial P}{\partial V} \right)_{V=V_0, T=0} \quad (4.3)$$

and B'_0 is its derivative with respect to pressure at the equilibrium volume, V_0 , and E_0 is the energy at V_0

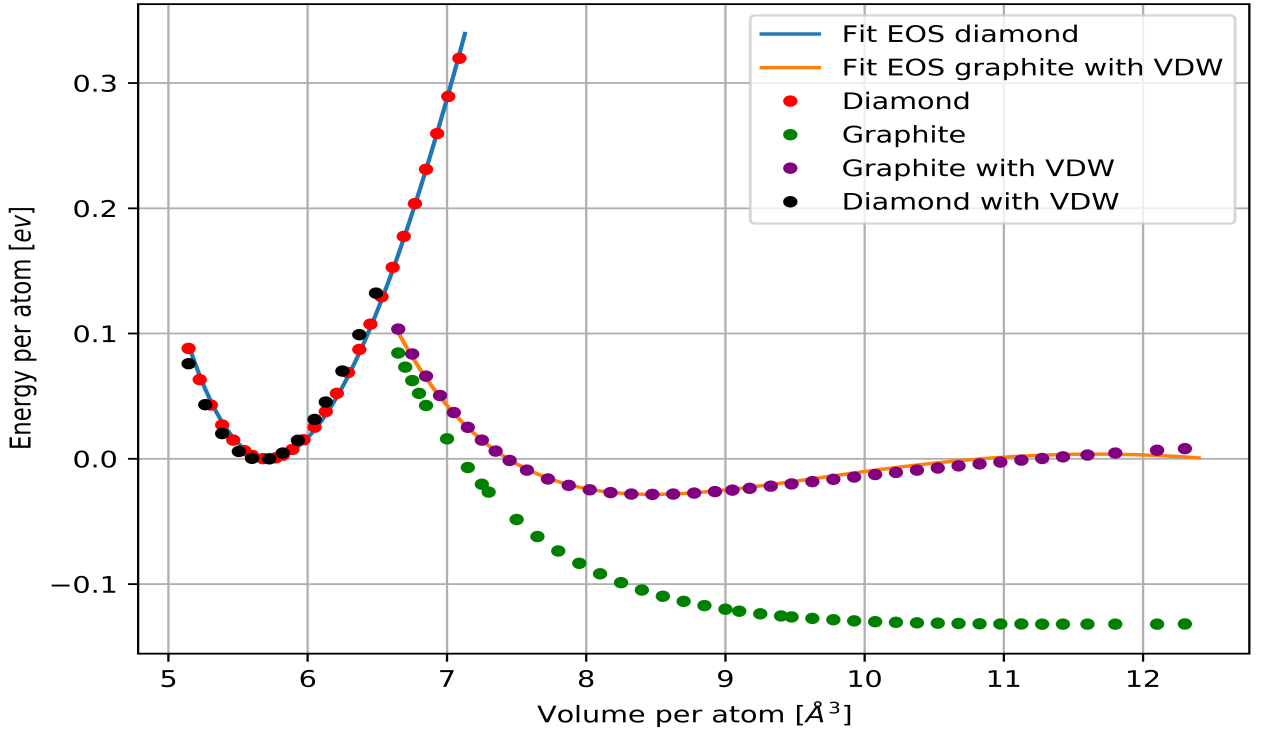


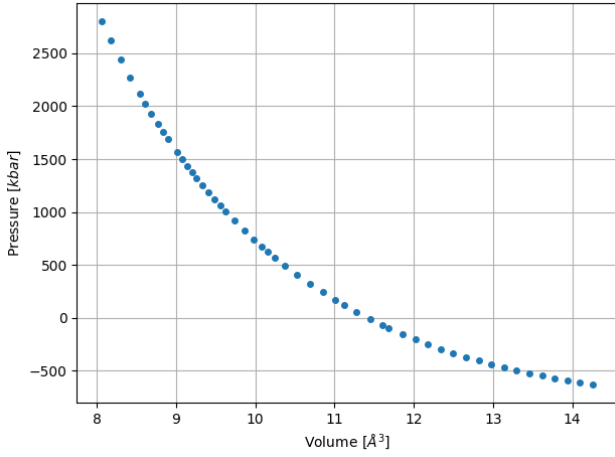
Figure 4: Energy-Volume curves

Below we include the values of the parameters B_0 and B'_0 obtained for each one of the numerical fits, in order to compare them with the experimental values:

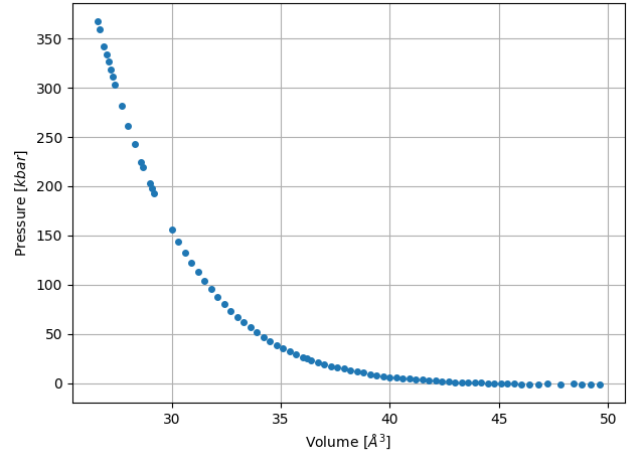
| | Numerical fit | | Experimental values [13] |
|-----------------|--------------------|----------------|--|
| Diamond | $B_0 = 430.14$ GPa | $B'_0 = 3.12$ | $B_0 = 442$ GPa |
| Graphite | $B_0 = 43.93$ GPa | $B'_0 = 10.95$ | $B_0 = -$ GPa |

Table 1: Comparison between the numerical fits and the experimental values.

Using the same data already produced by the simulations, we can also plot pressure-volume graphs for diamond and graphite, which allow us to gain a deeper insight into the physical behaviour of the studied materials:



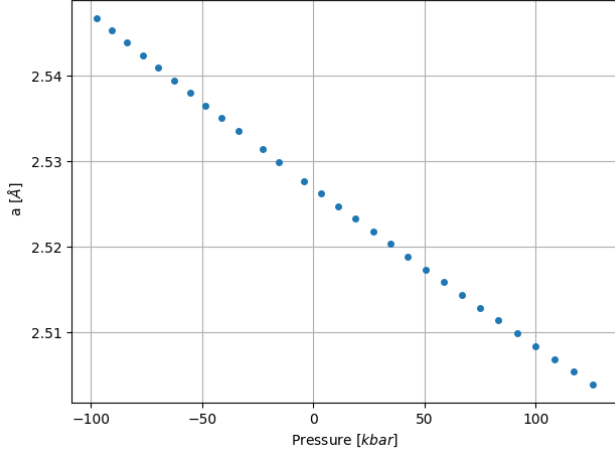
(a) P-V graph for diamond.



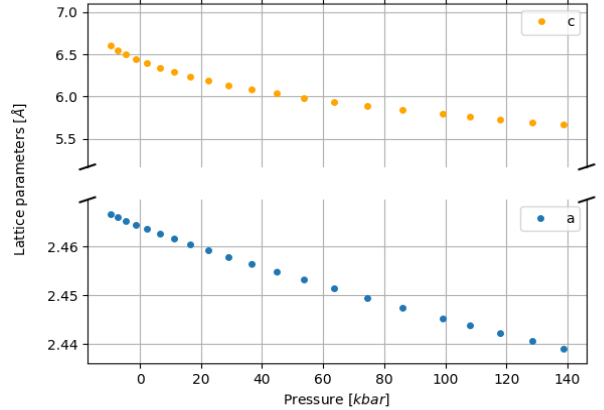
(b) P-V graph for graphite.

Figure 5: Pressure-volume graphs for diamond and graphite.

Using the same search technique already applied to obtain the pressure and energy data, we now search for the lattice parameters of the relaxed structure. It is important to note that, in the ionic relaxation, the process of generalized force minimization is constrained to a fixed selected volume. Studying the of this new set of data with pressure, we obtain the following graphs:



(a) Diamond.



(b) Graphite.

Figure 6: Lattice parameters evolution for diamond (left) and graphite (right)

Here we can observe how an increase on the volume of the cell entails a significative rise in the interplanar distance, c , while the parameter that represents the minimum distance between atoms, a , varies very slowly with pressure. Note that the relation between volume and pressure can be observed in the previous graphs, see 5. When it comes to diamond, the graph reveals that the lattice parameter decreases with an increase in pressure (equivalently, with a decrease in volume), as it is theoretically expected. In order to facilitate a comparison between the results obtained in the simulations with the experimental ones, we have elaborated the table that follows:

| | Simulations values at $T = 0\text{ K}$ | | Experimental values at $T = 298\text{ K}$ [13] | |
|-----------------|--|---------------------|--|---------------------|
| Diamond | $a = 2.53\text{ Å}$ | | $a = 3.57\text{ Å}$ | |
| Graphite | $a = 2.4\text{ Å}$ | $c = 5.28\text{ Å}$ | $a = 2.52\text{ Å}$ | $c = 4.12\text{ Å}$ |

Table 2: Comparison between the calculated lattice parameters and experimental values.

4.4.2 Electronic energy bands

In order to obtain the energy bands, it is necessary to split the necessary calculation in two parts. The first one consists in relaxing the structure so we can obtain the self-consistent charge density (VASP file: CHGCAR) for these structures. And secondly, using the relaxed structure (VASP file: CONTCAR) and the aforementioned self-consistent charge density, we repeat the simulations but this time without relaxing the structure and solving the Kohn-Sham equations for selected points in the FBZ. In this case the high-symmetry directions along which bands are going to be calculated are manually introduced, which can be seen in the following schematic figures:

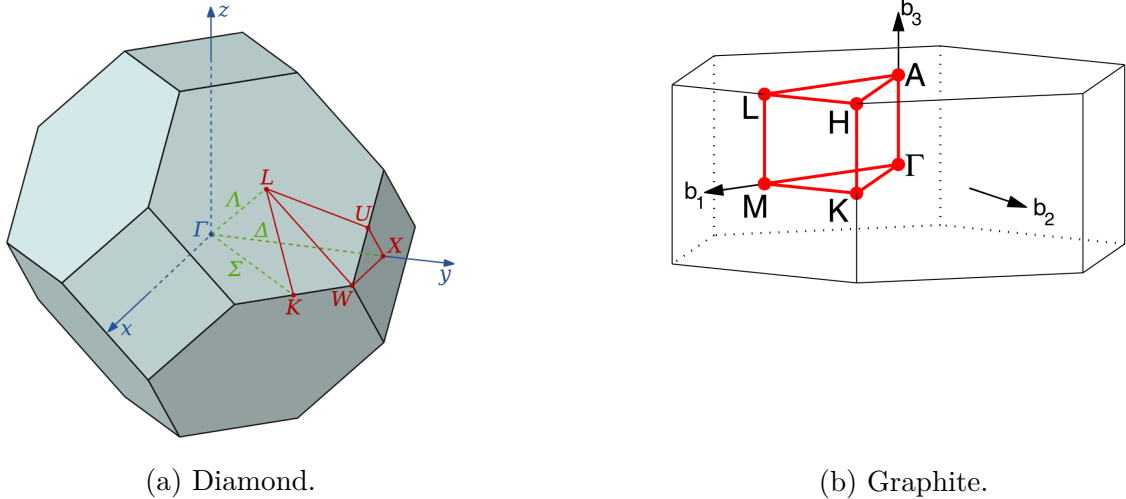


Figure 7: Brillouin zone and high symmetry directions for diamond [4] and graphite [4].

In these representations, as well as visualizing the energy bands, on the right margin of each graph we show the electronic density of states (DOS), which is defined as the number of electronic Kohn-Sham levels, $\epsilon_n(\vec{k})$, per volume in the \vec{k} -space, normalized to the volume of the crystal (given in arbitrary units). Here the number of bands used in order to elaborate the graphical representations has been limited, as the number of calculated bands is finite and this means that the visualization of the last bands would not be accurate, taking into account the overlapping between bands. It is also important to note that the origin of the energy is always taken at the maximum of the highest occupied band. This means that this origin coincides with the maximum of the eighth band in graphite, as each carbon atom contributes four electrons and there are four of these atoms in each conventional cell because each band (degenerated in spin) can only accept two electrons. Similarly, there are two carbon atoms in the unit cell of diamond, which means that the origin of energy coincides with the maximum of the fourth valence band.

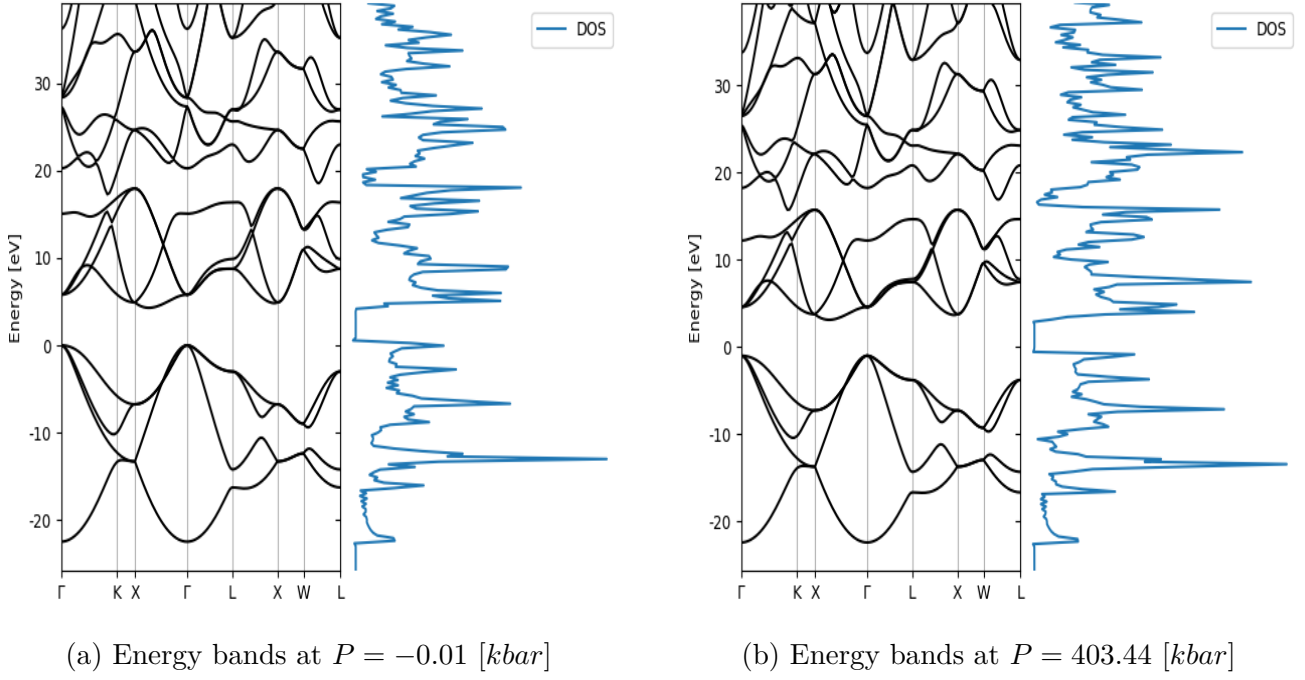


Figure 8: Energy bands on diamond.

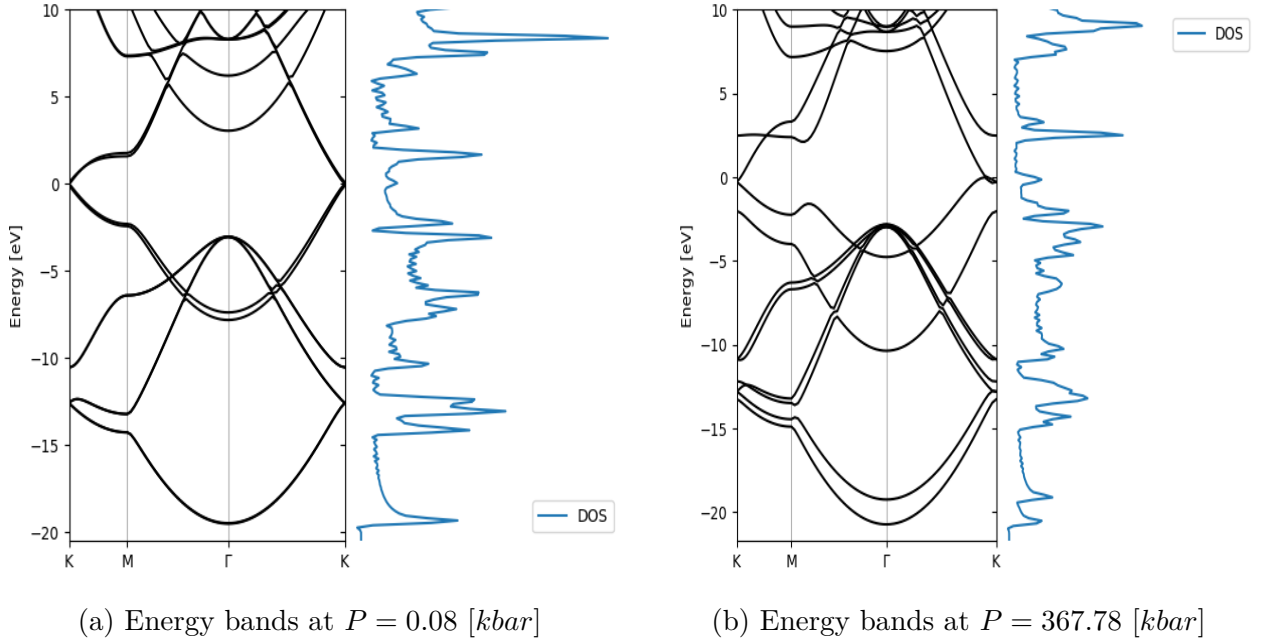


Figure 9: Energy bands on graphite.

When we analyze diamond we can observe the existence of an energy gap, where the density of states is null, as it can be seen on the representation of this density of states. We can also study the behaviour of the energy gap when the volume increases, which will be the opposite of the behaviour when the pressure increases, as it can be inferred from the pressure-volume graph presented before. It is important to take into account that the energy gap is measured as the difference between the maximum of the last occupied band (at the

zone center or Γ position in diamond) and the minimum of the first conduction band (in the $\Gamma - X$ direction). The described behaviour of the energy gap with volume and pressure is represented in the following plots:

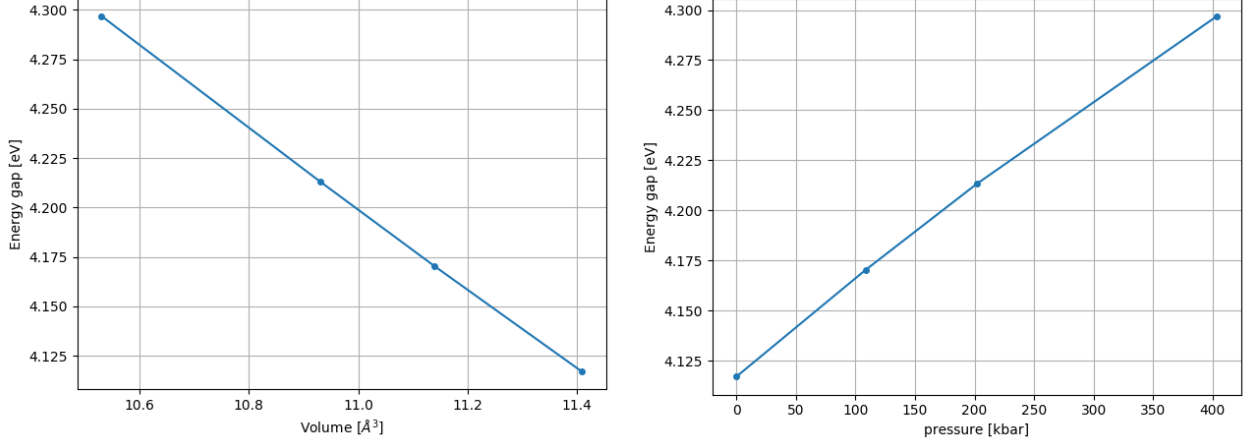


Figure 10: Evolution of the energy gap

Considering a fixed reference volume, that we choose among the ones used in the computational simulations so that is it as close as possible to the one for which experimental information is available, we can elaborate a table that allows us to compare the information generated by these simulations with the experimental results:

| | Calculated value at $T = 0$ K | Experimental values [13] |
|--------------------------------------|-------------------------------|---------------------------------|
| Indirect gap $E_{g,ind}$ [eV] | 4.12 – 4.3 | 5.48 at $T = 300$ K |
| $dE_{g,ind}/dp$ [eV/bar] | $4.5 \cdot 10^{-7}$ | $2 \cdot 10^{-7}$ at $T = 80$ K |

Table 3: Comparison between the numerical fits and the experimental values.

4.4.3 Electronic localization function (ELF)

The main underlying foundation of the electronic localization function (ELF) is the concept of Fermi's hole, i.e. the distribution of the probability of finding another electron in the neighborhood of a reference electron, when both have the same spin. Then, it is related to the concept of electronic localization function through the probability density for finding an electron with spin σ in \vec{r} when a second electron with spin σ' is situated in \vec{r}' . As it is out of the scope of this work, we will not explicitly derive the expression that results from the previous considerations:

$$ELF = (1 + \chi_\sigma^2)^{-1} \quad (4.4)$$

with:

$$\chi_\sigma = D_\sigma(\vec{r})/D_0(\vec{r}) \quad (4.5)$$

and

$$D_\sigma = \sum_{i=1}^N \left\| \vec{\nabla} \psi_i(\vec{r}) \right\|^2 - \frac{1}{4} \frac{\left\| \vec{\nabla} n(\vec{r}) \right\|}{n(\vec{r})} \quad \text{and} \quad D_0(\vec{r}) \propto n(\vec{r})^{5/3} \quad (4.6)$$

where $n(\vec{r})$ is the self-consistent electronic density described in previous sections. As far our calculations are concerned, it is only important to know that $0 \leq \text{ELF} \leq 1$, where values close to 1 means a high probability of finding the electron and values close to $1/2$ indicate a similar behaviour to the one exhibited by an electron gas. When it comes to the computational process involved in the computation of the ELF, it is quite similar to the one applied for the determination of the bands: the first part consists in a self-consistent calculation to relax the structure, and the second one allows us to compute the ELF using the already relaxed structure and charge density. These simulations generate the information contained in the following graphs for diamond and graphite:

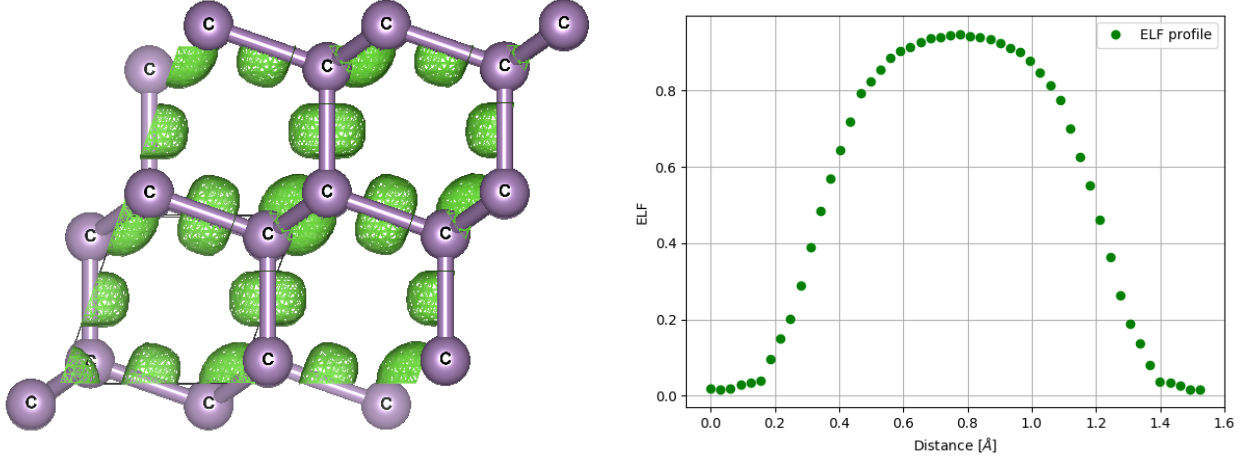


Figure 11: Electronic localization function (ELF) isosurface for $ELF = 0.75$ (left) and value of the ELF along the C-C bond for diamond (right).

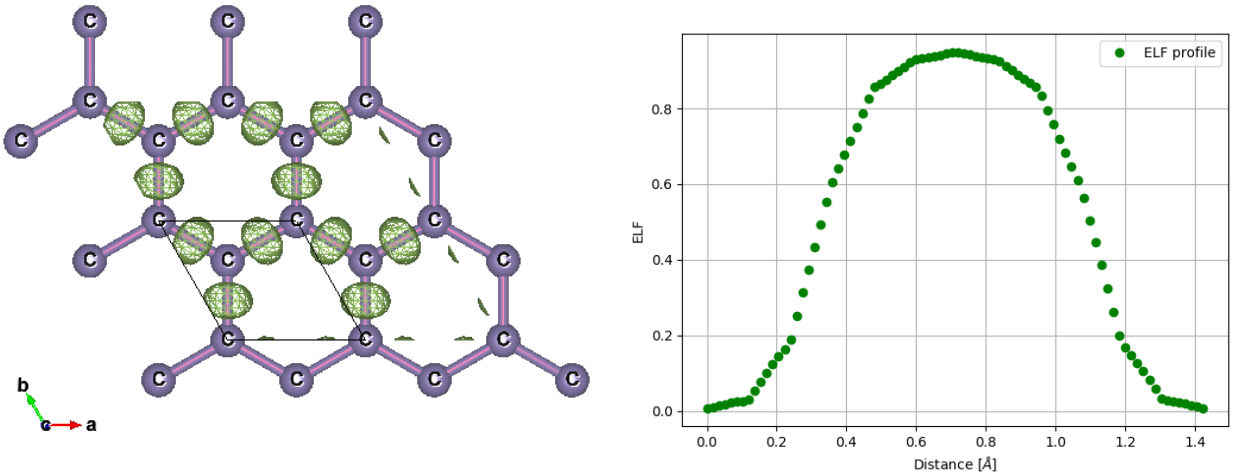


Figure 12: Electronic localization function (ELF) isosurface for $ELF = 0.86$ (left) and value of the ELF along the C-C bond for graphite (right).

These figures were elaborated from the raw data produced by the simulations, using the VESTA program and considering an isosurface of constant ELF. The distance between two of these atoms is 1.54 \AA for diamond and 1.4 \AA for graphite. In the case of both materials we can observe how the maximum electronic localization can be found in the interatomic position, which is indicative of a covalent bond. For further information, see [7] and [1].

5 Conclusions

In this work, the enormous efficacy of the density functional framework has become clear, both from a practical and a theoretical point of view, as it has allowed me to calculate various macroscopic parameters of solids within a fully quantum mechanical framework, and thus it has enabled me to compare theoretical predictions with experimental results. As we mentioned in the work, it was necessary to program a few Python scripts in order to parse all the raw outputs of the results of the calculations and represent them graphically. After this treatment and analysis of the data, we can conclude that the theoretical results underestimate the magnitude of the gap, which is a well-known feature of the Kohn-Sham theory, as it is a theory for the ground state and the gap involves excited states, not properly accounted for at this level. I have also studied the effect of the structure and symmetry of a material on its properties, by studying two phases of carbon, both with different properties.

This work has also allowed me to reinforce and expand my knowledge of Quantum Mechanics, as I not only had to understand the theoretical fundamentals of DFT, but also apply them to a practical situation, where as I commented before, can compare theoretical predictions and experimental results.

As a possible future extension of this work, I can mention the mathematical study of the role of the symmetry of a system on other properties, as well as a more in-depth analysis of the selected materials using different pseudopotentials and exchange-correlation potentials for the theoretical calculations, in order to check their impact on the final results, and a detailed study of the vibrational properties of both solids. Finally, this process could also be applied to the analysis of other interesting structures and materials.

A Appendix

A.1 Table of atomic units

In this appendix we present the usual units that are used along this work. The Hamiltonian [3.1] is written in Gaussian units, but there exist more ways to choose the system of units ⁴:

| <i>Expression of some fundamental constants</i> | | |
|---|--|---|
| $a_B = \frac{\hbar^2}{me^2} = \text{Bohr radius} = 0.529 \text{ \AA}$ | $1 \text{ Rydberg} = \frac{\hbar^2}{2ma_B^2} = \frac{e^2}{2a_B} = 13.606 \text{ eV}$ | |
| $\alpha^{-1} = \frac{\hbar c}{e^2} = 137.036$ | $1 \text{ Hartree} = \frac{e^2}{a_B} = 27.21 \text{ eV}$ | |
| <i>Hartree atomic units:</i> $\hbar = 1$ $m = 1$ $e = 1$ | | |
| unit of length = a_B | unit of energy = 1 Hartree | velocity of light = α^{-1} |
| <i>Rydberg atomic units:</i> $\hbar = 1$ $m = 1/2$ $e^2 = 2$ | | |
| unit of length = a_B | unit of energy = 1 Rydberg | velocity of light = $2 \cdot \alpha^{-1}$ |

A.2 Bloch's theorem for the multidimensional case

In this appendix we are going to derive Bloch's theorem for the multidimensional case. The proof is based on the translational symmetry of the system and the bounded character of the wave functions.

Theorem. The solutions of the time-independent Schrödinger equation for a particle in a periodic external field:

$$\hat{H} = -\Delta + V(\vec{r}) \quad \text{with} \quad V(\vec{r} + \vec{R}) = V(\vec{r}) \quad \vec{R} \in \mathbf{R} \quad (\text{A.1})$$

have the form:

$$\psi_{\vec{k}}(\vec{r}) = e^{i\vec{k} \cdot \vec{r}} u_{\vec{k}}(\vec{r}) \quad (\text{A.2})$$

Proof. As long as the system has translational symmetry, the Hamiltonian commutes with translations, i.e.:

$$[\hat{H}, T_{\vec{R}}] = 0 \quad (\text{A.3})$$

Therefore, the translations and the Hamiltonian have common eigenvectors:

$$\left. \begin{aligned} \hat{H}\psi &= E\psi \\ T_{\vec{R}}\psi &= c(\vec{R})\psi \end{aligned} \right\} \quad (\text{A.4})$$

The key point in all of this proof is to find out which are the eigenvalues of the translation operator using its properties. Let's consider the action of two different translations on an eigenvector, $T_{\vec{R}}$ and $T_{\vec{R}'}$. On one hand we get:

$$T_{\vec{R}}T_{\vec{R}'}\psi = c(\vec{R})c(\vec{R}')\psi \quad (\text{A.5})$$

⁴This figure is extracted from [8], p. 190.

On the other hand, $T_{\vec{R}}T_{\vec{R}'}$ is a translation in the direction of $\vec{R} + \vec{R}'$:

$$T_{\vec{R}}T_{\vec{R}'}\psi = T_{\vec{R}+\vec{R}'}\psi = c(\vec{R} + \vec{R}')\psi \quad (\text{A.6})$$

Therefore, the eigenvalues of the translation operator satisfy:

$$c(\vec{R} + \vec{R}') = c(\vec{R})c(\vec{R}') \quad (\text{A.7})$$

For each translation on the direction of a lattice generator (\vec{a}_i), see [3.51], we can write:

$$c(\vec{a}_i) = e^{i2\pi x_i} \quad (\text{A.8})$$

Hence, in the general case, where $\vec{R} = \sum_{i=1}^3 n_i \vec{a}_i$, we define:

$$\vec{k} = \sum_{i=1}^3 x_i \vec{b}_i \quad \text{with:} \quad \vec{a}_i \cdot \vec{b}_j = 2\pi \delta_{ij} \quad (\text{A.9})$$

So, the general form of the eigenvectors of the translation operators is:

$$c(\vec{R}) = e^{i\vec{k} \cdot \vec{R}} \quad (\text{A.10})$$

Hence, recalling the definition of c [A.4]:

$$\psi(\vec{r} + \vec{R}) = e^{i\vec{k} \cdot \vec{R}} \psi(\vec{r}) \quad (\text{A.11})$$

Claim. The function:

$$u_{\vec{k}}(\vec{r}) = e^{-i\vec{k} \cdot \vec{r}} \psi(\vec{r}) \quad (\text{A.12})$$

is periodic, i.e. $u_{\vec{k}}(\vec{r} + \vec{R}) = u_{\vec{k}}(\vec{r})$.

Proof. We just need to substitute directly into the definition of u and take into account the former result:

$$u_{\vec{k}}(\vec{r} + \vec{R}) = e^{-i\vec{k} \cdot \vec{r}} e^{-i\vec{k} \cdot \vec{R}} \psi(\vec{r} + \vec{R}) = e^{-i\vec{k} \cdot \vec{r}} e^{-i\vec{k} \cdot \vec{R}} e^{i\vec{k} \cdot \vec{R}} \psi(\vec{r}) = e^{-i\vec{k} \cdot \vec{r}} \psi(\vec{r}) \quad (\text{A.13})$$

which concludes the proof.

Then, if we solve the last equation for ψ we get:

$$\psi(\vec{r}) = e^{i\vec{k} \cdot \vec{r}} u_{\vec{k}}(\vec{r}) \quad (\text{A.14})$$

which is the desired result. \square

A.3 Some explicit calculations related to the electron density

The aim of this appendix is to ascertain all the relations related to the electron density, given along this work without proof.

Let's consider the expectation value of an operator \hat{F} as to a state $\Psi(\vec{r}_1, \vec{r}_2, \dots, \vec{r}_N)$:

$$\langle \hat{F} \rangle_{\Psi} = \frac{\langle \Psi | \hat{F} | \Psi \rangle}{\langle \Psi | \Psi \rangle} \quad (\text{A.15})$$

with \hat{F} of the form:

$$\hat{F} = \sum_{i=1}^N \hat{f}(\vec{r}; \vec{r}_i) \quad (\text{A.16})$$

where \vec{r}_i are the spatial coordinates of each particle of the system and \hat{f} acts multiplicatively on Ψ . Without loss of generality, we are going to consider that the state Ψ is normalized to one, since the normalized constant can be absorbed by \hat{f} . Inserting these considerations into [A.29]:

$$\left\langle \Psi \left| \sum_{i=1}^N \hat{f}(\vec{r}; \vec{r}_i) \right| \Psi \right\rangle = \sum_{i=1}^N \int \Psi^*(\vec{r}_1, \vec{r}_2, \dots, \vec{r}_N) \hat{f}(\vec{r}; \vec{r}_i) \Psi(\vec{r}_1, \vec{r}_2, \dots, \vec{r}_N) d^3 r_1 d^3 r_2 \dots d^3 r_N = \quad (\text{A.17})$$

$$= \sum_{i=1}^N \int \hat{f}(\vec{r}; \vec{r}_i) \left[\int \Psi^*(\vec{r}_1, \vec{r}_2, \dots, \vec{r}_N) \Psi(\vec{r}_1, \vec{r}_2, \dots, \vec{r}_N) d^3 r_1 d^3 r_2 \dots d^3 r_N \right] d^3 r_i = \quad (\text{A.18})$$

The integration over the \vec{r}_i spatial coordinate does not depend on i , because \vec{r}_i is just a dummy variable, so we can just change its label by \vec{r}' :

$$= \sum_{i=1}^N \int \hat{f}(\vec{r}; \vec{r}') \left[\int \Psi^*(\vec{r}_1, \vec{r}_2, \dots, \vec{r}_N) \Psi(\vec{r}_1, \vec{r}_2, \dots, \vec{r}_N) d^3 r_1 d^3 r_2 \dots d^3 r_N \right] d^3 r' = \quad (\text{A.19})$$

$$= \int \hat{f}(\vec{r}; \vec{r}') \left[N \int \Psi^*(\vec{r}_1, \vec{r}_2, \dots, \vec{r}_N) \Psi(\vec{r}_1, \vec{r}_2, \dots, \vec{r}_N) d^3 r_1 d^3 r_2 \dots d^3 r_N \right] d^3 r' \quad (\text{A.20})$$

By means of measurement we cannot distinguish which particle is being measured, and the wave function must have a well-defined behaviour under an interchange of particles:

$$\Psi(\vec{r}_1, \vec{r}_2, \dots, \vec{r}_i, \dots, \vec{r}_j, \dots, \vec{r}_N) = \pm \Psi(\vec{r}_1, \vec{r}_2, \dots, \vec{r}_j, \dots, \vec{r}_i, \dots, \vec{r}_N) \quad (\text{A.21})$$

In eq. A.20 we can interchange the first and the i -th position vectors and relabel all the integration variables:

$$= \int \hat{f}(\vec{r}; \vec{r}') \underbrace{\left[N \int \Psi^*(\vec{r}', \vec{r}_2, \dots, \vec{r}_N) \Psi(\vec{r}', \vec{r}_2, \dots, \vec{r}_N) d^3 r_2 \dots d^3 r_N \right]}_{n(\vec{r}')} d^3 r' \quad (\text{A.22})$$

Hence, the expectation value of \hat{F} as to Ψ :

$$\langle \hat{F} \rangle_{\Psi} = \int \hat{f}(\vec{r}; \vec{r}') \cdot n(\vec{r}') d^3 r' \quad (\text{A.23})$$

Eq. [3.5] and [3.11] can be proven by means of this result. Let's consider the density operator:

$$\hat{n} = \sum_{i=1}^N \delta(\vec{r} - \vec{r}_i) \quad \hat{f}(\vec{r}; \vec{r}_i) = \delta(\vec{r} - \vec{r}_i) \quad (\text{A.24})$$

The expectation value of the density operator is the electron density:

$$n(\vec{r}) = \langle \hat{n} \rangle_{\Psi} = \int \delta(\vec{r} - \vec{r}') \cdot n(\vec{r}') d^3 r' = N \int \Psi^*(\vec{r}, \vec{r}_2, \dots, \vec{r}_N) \Psi(\vec{r}', \vec{r}_2, \dots, \vec{r}_N) d^3 r_2 \dots d^3 r_N \quad (\text{A.25})$$

The expectation value of the external potential trivially follows from the former result:

$$\left\langle \Psi \left| \sum_{i=1}^N v_{ext}(\vec{r}_i) \right| \Psi \right\rangle = \int v_{ext}(\vec{r}) \cdot n(\vec{r}) d^3r \quad (\text{A.26})$$

From now on in we will consider a system of non-interacting fermions. The wave function of such a system must be antisymmetric as to an interchange of particles, and we take it as an Slater determinant:

$$\Psi(\vec{r}_1, \vec{r}_2, \dots, \vec{r}_N) = \frac{1}{\sqrt{N!}} \cdot \det \begin{pmatrix} \psi_1(\vec{r}_1) & \psi_2(\vec{r}_1) & \cdots & \psi_N(\vec{r}_1) \\ \psi_1(\vec{r}_2) & \psi_2(\vec{r}_2) & \cdots & \psi_N(\vec{r}_2) \\ \vdots & \vdots & \ddots & \vdots \\ \psi_1(\vec{r}_N) & \psi_2(\vec{r}_N) & \cdots & \psi_N(\vec{r}_N) \end{pmatrix} \quad (\text{A.27})$$

Instead of using the determinant notation, we will use an expanded version of it:

$$\Psi(\vec{r}_1, \vec{r}_2, \dots, \vec{r}_N) = \frac{1}{\sqrt{N!}} \sum_{\sigma \in \Pi_N} \epsilon_\sigma \cdot \psi_{\sigma_1}(\vec{r}_1) \cdot \psi_{\sigma_2}(\vec{r}_2) \cdots \psi_{\sigma_N}(\vec{r}_N) \quad (\text{A.28})$$

where Π_N is the symmetric group of degree N , σ_i is the i -th slot of the array $\sigma \in \Pi_N$ and $\epsilon_\sigma = \pm 1$ is its parity.

Let's consider again the expectation value of an operator \hat{F} as to a state $\Psi(\vec{r}_1, \vec{r}_2, \dots, \vec{r}_N)$:

$$\langle \hat{F} \rangle_\Psi = \frac{\langle \Psi | \hat{F} | \Psi \rangle}{\langle \Psi | \Psi \rangle} \quad (\text{A.29})$$

with \hat{F} of the form:

$$\hat{F} = \sum_{i=1}^N \hat{f}(\vec{r}; \vec{r}_i) \quad (\text{A.30})$$

where \vec{r}_i are the spatial coordinates of each particle of the system and \hat{f} does not act multiplicatively on Ψ .

$$\left\langle \Psi \left| \sum_{i=1}^N \hat{f}(\vec{r}; \vec{r}_i) \right| \Psi \right\rangle = \frac{1}{N!} \sum_{i=1}^N \sum_{\sigma \in \Pi_N} \sum_{\gamma \in \Pi_N} \epsilon_\sigma \epsilon_\gamma \langle \psi_{\sigma_1} \cdots \psi_{\sigma_N} | \hat{f}(\vec{r}; \vec{r}_i) | \psi_{\gamma_1} \cdots \psi_{\gamma_N} \rangle = \quad (\text{A.31})$$

$$= \frac{1}{N!} \sum_{i=1}^N \sum_{\sigma \in \Pi_N} \sum_{\gamma \in \Pi_N} \epsilon_\sigma \epsilon_\gamma \int \psi_{\sigma_1}^*(\vec{r}_1) \cdots \psi_{\sigma_N}^*(\vec{r}_N) \hat{f}(\vec{r}; \vec{r}_i) \psi_{\gamma_1}(\vec{r}_1) \cdots \psi_{\gamma_N}(\vec{r}_N) d^3r_1 \cdots d^3r_N = \quad (\text{A.32})$$

$$= \frac{1}{N!} \sum_{i=1}^N \sum_{\sigma \in \Pi_N} \sum_{\gamma \in \Pi_N} \epsilon_\sigma \epsilon_\gamma \delta_{\sigma_1, \gamma_1} \cdots \int \psi_{\sigma_i}^*(\vec{r}_i) \hat{f}(\vec{r}; \vec{r}_i) \psi_{\gamma_i}(\vec{r}_i) d^3r_i \cdots \delta_{\sigma_N, \gamma_N} \quad (\text{A.33})$$

Each term of the sum vanishes except for those permutations $\gamma \in \Pi_N$, whose i -th element differs from the i -th elements of $\sigma \in \Pi_N$. We now inquire as to that different element. Let's remember the definition of a permutation:

$$\begin{pmatrix} 1 & 2 & 3 & \cdots & i & \cdots & N \\ \sigma_1 & \sigma_2 & \sigma_3 & \cdots & \sigma_i & \cdots & \sigma_N \end{pmatrix} \stackrel{?}{=} \begin{pmatrix} 1 & 2 & 3 & \cdots & i & \cdots & N \\ \gamma_1 & \gamma_2 & \gamma_3 & \cdots & \gamma_i & \cdots & \gamma_N \end{pmatrix} \quad (\text{A.34})$$

The second row contains all the natural numbers up to N ordered in all possible ways. If all the terms of both permutations are the same, except for i -th element, which is unknown, the permutations are identical. Inserting this consideration and relabelling the integration variable ⁵:

$$= \frac{1}{N!} \sum_{i=1}^N \sum_{\sigma \in \Pi_N} \int \psi_{\sigma_i}^*(\vec{r}') \cdot \hat{f}(\vec{r}; \vec{r}') \cdot \psi_{\sigma_i}(\vec{r}') d^3 r' \quad (\text{A.35})$$

We must bear in mind that σ_i is just the i -th slot of the permutation, and there are $(N-1)!$ permutations with the same element at the i -th slot:

$$= \frac{1}{N!} \sum_{i=1}^N \left[(N-1)! \sum_{j=1}^N \int \psi_j^*(\vec{r}) \cdot \hat{f}(\vec{r}; \vec{r}_i) \cdot \psi_j(\vec{r}) d^3 r \right] = \sum_{j=1}^N \int \psi_j^*(\vec{r}) \cdot \hat{f}(\vec{r}; \vec{r}_i) \cdot \psi_j(\vec{r}) d^3 r \quad (\text{A.36})$$

Hence, the expectation value of \hat{F} as to Ψ is:

$$\left\langle \Psi \left| \sum_{i=1}^N \hat{f}(\vec{r}; \vec{r}_i) \right| \Psi \right\rangle = \sum_{i=1}^N \langle \psi_i | \hat{f}(\vec{r}; \vec{r}_i) | \psi_i \rangle \quad (\text{A.37})$$

Thus, the electron density of non-interacting system is:

$$n(\vec{r}) = \langle \hat{n} \rangle_{\Psi} = \sum_{i=1}^N \langle \psi_i | \delta(\vec{r} - \vec{r}') | \psi_i \rangle = \sum_{i=1}^N \psi_i^*(\vec{r}) \psi_i(\vec{r}) \quad (\text{A.38})$$

The expectation value of the kinetic energy of the non-interacting system follows from the previous result:

$$T_o[n] = \langle \Psi | \hat{T} | \Psi \rangle = \sum_{i=1}^N \langle \psi_i | \hat{T} | \psi_i \rangle \quad (\text{A.39})$$

A.4 Derivation of the Kohn-Sham equations

In this appendix we are going to derive explicitly the Kohn-Sham equations. Let us consider the functional:

$$\begin{aligned} E^{(HS)} \left[\{\phi_i\}_{i=1}^N, \{\phi_i^*\}_{i=1}^N \right] &= \sum_{i=1}^N \langle \phi_i | \hat{T} | \phi_i \rangle + \frac{1}{2} \int \frac{n(\vec{r})n(\vec{r}')}{|\vec{r} - \vec{r}'|} d^3 r d^3 r' + \\ &+ \int V_{nucl}(\vec{r}) \cdot n(\vec{r}) d^3 r + E_{xc}[n] \end{aligned} \quad (\text{A.40})$$

subjected to orthonormalization constrains:

$$\int \phi_i(\vec{r}) \phi_j(\vec{r}) d^3 r = \delta_{ij} \quad (\text{A.41})$$

and with:

$$n(\vec{r}) = \sum_{i=1}^N \phi_i(\vec{r}) \phi_i^*(\vec{r}) \quad (\text{A.42})$$

⁵If both permutations are the same, the parity too, so $\epsilon_{\sigma}^2 = 1$

We introduce a set of Lagrange multipliers $\{\lambda_{ij}\}_{i,j=1}^N$ in order to take into account the former constraints:

$$F[\{\phi_i\}_{i=1}^N, \{\phi_i^*\}_{i=1}^N] = E^{(HS)}[\{\phi_i\}_{i=1}^N, \{\phi_i^*\}_{i=1}^N] - \sum_{i=1}^N \sum_{j=1}^N \lambda_{ij} \left[\int \phi_i^*(\vec{r}) \phi_j(\vec{r}) d^3r - 1 \right] \quad (\text{A.43})$$

From the variational principle it follows that the first order variation of F with respect to any state ϕ_k must be zero:

$$\delta F := F[\{\phi_i\}_{i=1}^N, \{\phi_i^*\}_{i \neq k}^N, \phi_k^* + \delta \phi_k^*] - F[\{\phi_i\}_{i=1}^N, \{\phi_i^*\}_{i=1}^N] = 0 \quad (\text{A.44})$$

We are going to compute the variation of each term separately.

The variation of the first term is easy to compute as long that the only term that remains occurs when the index of the sum is k , and the rest cancel out when we perform the variation:

$$\delta[1]_1 = \sum_{i \neq k}^N \int \phi_i^*(\vec{r}) \hat{T} \phi_i(\vec{r}) d^3r + \int [\phi_k^*(\vec{r}) + \delta \phi_k^*(\vec{r})] \hat{T} \phi_k(\vec{r}) d^3r - \sum_{i=1}^N \int \phi_i^*(\vec{r}) \hat{T} \phi_i(\vec{r}) d^3r \quad (\text{A.45})$$

where $\delta[1]_1$ indicates that we are taking the variation of the first term of equation [1]. Then, the last equation is reduced to:

$$\delta[1]_1 = \int \delta \phi_k^*(\vec{r}) [\hat{T} \phi_k(\vec{r})] d^3r \quad (\text{A.46})$$

The computation of the second term must be done carefully because in the double sum the state ϕ_k appears more than one time. First, if $i \neq k$ in the j sum, then the term $\delta \phi_k^*$ appears one time. Similarly, for $i = j$ the term appears again, and also in the case $i = j = k$. We will just sketch the relevant terms of the calculations:

$$i = k, \forall j \neq k : \sum_{j \neq k}^N \int \frac{[\phi_k^*(\vec{r}) + \delta \phi_k^*(\vec{r})] \phi_k(\vec{r}) \phi_j^*(\vec{r}') \phi_j(\vec{r}')}{|\vec{r} - \vec{r}'|} d^3r d^3r' \longrightarrow \quad (\text{A.47})$$

$$\text{The only relevant term} \longrightarrow \int \delta \phi_k^*(\vec{r}) \left[\int \frac{\sum_{j \neq k}^N \phi_j^*(\vec{r}') \phi_j(\vec{r}')}{|\vec{r} - \vec{r}'|} d^3r' \right] \phi_k(\vec{r}) d^3r \quad (\text{A.48})$$

Similarly we have:

$$j = k, \forall i \neq k : \sum_{i \neq k}^N \int \frac{\phi_i^*(\vec{r}) \phi_i(\vec{r}) [\phi_k^*(\vec{r}') + \delta \phi_k^*(\vec{r}')] \phi_k(\vec{r}')}{|\vec{r} - \vec{r}'|} d^3r d^3r' \longrightarrow \quad (\text{A.49})$$

$$\text{The only relevant term} \longrightarrow \int \delta \phi_k^*(\vec{r}') \left[\int \frac{\sum_{i \neq k}^N \phi_i^*(\vec{r}) \phi_i(\vec{r})}{|\vec{r} - \vec{r}'|} d^3r \right] \phi_k(\vec{r}') d^3r' \quad (\text{A.50})$$

Finally, the term with $i = j = k$:

$$\int \frac{[\phi_k^*(\vec{r}) + \delta \phi_k^*(\vec{r})] \phi_k(\vec{r}) [\phi_k^*(\vec{r}') + \delta \phi_k^*(\vec{r}')] \phi_k(\vec{r}')}{|\vec{r} - \vec{r}'|} d^3r d^3r' \longrightarrow \quad (\text{A.51})$$

$$\text{The only relevant terms} \longrightarrow \int \delta \phi_k^*(\vec{r}') \left[\int \frac{\phi_k^*(\vec{r}) \phi_k(\vec{r})}{|\vec{r} - \vec{r}'|} d^3r \right] \phi_k(\vec{r}') d^3r' +$$

$$+ \int \delta\phi_k^*(\vec{r}) \left[\int \frac{\phi_k^*(\vec{r}')\phi_k(\vec{r}')}{|\vec{r}-\vec{r}'|} d^3r' \right] \phi_k(\vec{r}) d^3r + o(\delta\phi_k^*)^2 \quad (\text{A.52})$$

Thus, the first order variation of the second term of [1] is:

$$\delta[1]_2 = \int \delta\phi_k^*(\vec{r}) \left[\int \frac{n(\vec{r}')}{|\vec{r}-\vec{r}'|} d^3r' \right] \phi_k(\vec{r}) d^3r \quad (\text{A.53})$$

The variation of the third term is easy to calculate, and so we just give the result:

$$\delta[1]_3 = \int \delta\phi_k^*(\vec{r}) V_{nucl}(\vec{r}) \phi_k(\vec{r}) d^3r \quad (\text{A.54})$$

and by definition of functional derivative, the variation of the last term is:

$$\delta[1]_4 = \int \delta\phi_k^*(\vec{r}) \cdot \left(\frac{\delta E_{xc}}{\delta\phi_k^*} \right) d^3r = \int \delta\phi_k^*(\vec{r}) \left(\frac{\delta E_{xc}}{\delta n} \right) \phi_k(\vec{r}) d^3r \quad (\text{A.55})$$

where we applied the analog to the chain rule to the functional derivative.

Finally, to compute the variation of the last term of eq. [4] we only have to bear in mind that the only contribution to the variation appears when $i=k$:

$$\delta[4]_2 = \int \delta\phi_k^*(\vec{r}) \left[\sum_{j=1}^N \lambda_{kj} \cdot \phi_j(\vec{r}) \right] d^3r \quad (\text{A.56})$$

Therefore, the total variation of F is:

$$\delta F = \int \delta\phi_k^*(\vec{r}) \left[\hat{T} \phi_k(\vec{r}) + \left[\int \frac{n(\vec{r}')}{|\vec{r}-\vec{r}'|} d^3r' \right] \phi_k(\vec{r}) + V_{nucl}(\vec{r}) \phi_k(\vec{r}) + \left(\frac{\delta E_{xc}}{\delta n} \right) \phi_k(\vec{r}) - \sum_{j=1}^N \lambda_{kj} \cdot \phi_j(\vec{r}) \right] d^3r = 0 \quad (\text{A.57})$$

Hence, since the variation $\delta\phi_k^*$ is arbitrary, the terms inside the brackets must be zero:

$$\underbrace{\left[\hat{T} + \int \frac{n(\vec{r}')}{|\vec{r}-\vec{r}'|} d^3r' + V_{nucl}(\vec{r}) + \left(\frac{\delta E_{xc}}{\delta n} \right) \right]}_{F^{(KS)}} \phi_i(\vec{r}) = \sum_{j=1}^N \lambda_{ij} \cdot \phi_j(\vec{r}) \quad (\text{A.58})$$

Let's consider a non-degenerate linear transformation Λ independent of the coordinates such that:

$$\phi_i(\vec{r}) = \sum_{j=1}^N \Lambda_{ij} \psi_j(\vec{r}) \quad (\text{A.59})$$

Applying this transformation to the last equation:

$$F^{(KS)} \psi_n(\vec{r}) = \sum_{k=1}^N \left[\sum_{j=1}^N \sum_{k=1}^N \Lambda_{ni}^{-1} \lambda_{ij} \Lambda_{jk} \right] \psi_k(\vec{r}) \quad (\text{A.60})$$

We impose that the transformation Λ is such that the the terms of the matrix multiplication in brackets are the element of a diagonal matrix:

$$F^{(KS)} \psi_n(\vec{r}) = \varepsilon_n \psi_n(\vec{r}) \quad (\text{A.61})$$

Notice that the existence of such a matrix Λ that makes the matrix λ diagonal is a consequence of the hermiticity of $F^{(KS)}$, so its eigenvectors are orthogonal, and then the orthogonalization constraint [2] can be relaxed to just a normalization constraints, which implies the last result.

References

- [1] Castep. Available at <https://www.tcm.phy.cam.ac.uk/castep/documentation/WebHelp/content/modules/castep/thcastepelf.htm>.
- [2] Vasp official site. Available at <https://cms.mpi.univie.ac.at/vasp/vasp/vasp.html>.
- [3] Vesta official site. Available at <https://cms.mpi.univie.ac.at/vasp/vasp/vasp.html>.
- [4] Wikipedia. Available at https://en.m.wikipedia.org/wiki/Brillouin_zone.
- [5] N.W. Ashcroft and N.D. Mermin. *Solid State Physics*. Cengage Learning, 2011.
- [6] Dr. Robert E. Belford. Crystal lattices and unit cells. Available at https://chem.libretexts.org/Courses/University_of_Arkansas_Little_Rock/Chem_1403%3A_General_Chemistry_2/Text/12%3A_Solids/12.1_Crystal_Lattices_and_Unit_Cells.
- [7] Patricio Fuentealba, E. Chamorro, and Juan C. Santos. Chapter 5 understanding and using the electron localization function. In Alejandro Toro-Labbé, editor, *Theoretical Aspects of Chemical Reactivity*, volume 19 of *Theoretical and Computational Chemistry*, pages 57 – 85. Elsevier, 2007.
- [8] G. Grosso and G.P. Parravicini. *Solid State Physics*. Elsevier Science, 2000.
- [9] P. Hohenberg and W. Kohn. Inhomogeneous electron gas. *Phys. Rev.*, 136:B864–B871, Nov 1964.
- [10] Jorge Kohanoff. *Electronic Structure Calculations for Solids and Molecules: Theory and Computational Methods*. Cambridge University Press, 2006.
- [11] W. Kohn. Nobel lecture: Electronic structure of matter—wave functions and density functionals. *Rev. Mod. Phys.*, 71:1253–1266, Oct 1999.
- [12] W. Kohn and L. J. Sham. Self-consistent equations including exchange and correlation effects. *Phys. Rev.*, 140:A1133–A1138, Nov 1965.
- [13] H. Landolt, R. Börnstein, H. Fischer, O. Madelung, and G. Deuschle. *Landolt-Bornstein: Numerical Data and Functional Relationships in Science and Technology*. Number v. 17 in Numerical Data and Functional Relationships in Science and Technology Series. Springer, 1987.
- [14] D.E. Sands. *Introduction to Crystallography*. Dover Books on Chemistry Series. Dover Publications, 1993.
- [15] Dr. Frederic P. Schuller. Lectures on quantum theory. Available at <https://www.video.uni-erlangen.de/clip/id/5280>.